TU WIEN

TECHNISCHE UNIVERSITÄT WIEN

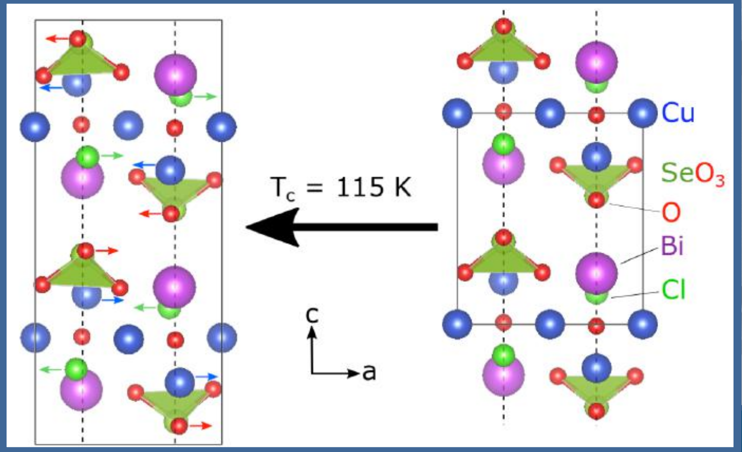

Francisite: a candidate “antiferroelectric” multiferroic

Evan Constable, L. Bergen, L. Weymann, E. Malysheva, A. Pimenov - Institute for solid state physics, TU Wien, Austria.

M. Guennou, C. Milesi-Brault, C. Toulouse, H. Aramberri, J. Íñiguez - Luxembourg Institute of Science and Technology / University of Luxembourg, Luxembourg.

J. Debray, S. deBrion, V. Simonet - Institut Néel, CNRS, Université Grenoble Alpes, France.

S. Raymond, E. Ressouche, F. Bourdarot - INAC, CEA and Université Grenoble Alpes France.

L. Paolasini, A. Bosak - European Synchrotron Radiation Facility, Grenoble, France.

S. Petit - Laboratoire Léon Brillouin, CEA, CNRS, Université Paris-Saclay, France.

H. Berger - Institute of Physics, Ecole Polytechnique Fédéral de Lausanne, Switzerland.

NÉEL institut · cnrs · UNIVERSITÉ Grenoble Alpes · LLB Orphée Laboratoire Léon Brillouin · cea · ILL NEUTRONS FOR SCIENCE · uni.lu UNIVERSITÉ DU LUXEMBOURG · LUXEMBOURG INSTITUTE OF SCIENCE AND TECHNOLOGY LIST

Francisite: mais ce n’est pas français…

CuBi(SeO$_3$)$_2$O$_2$Cl… or simply **CBSCl**

Iron monarch (open cut mine), Iron Knob, South Australia

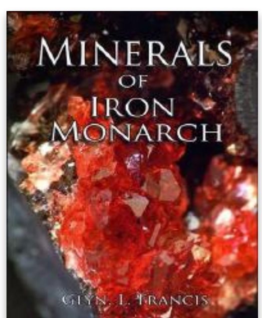

Original ore specimen submitted by Glyn Francis in 1987.

Previously unidentified CuBi(SeO$_3$)$_2$O$_2$Cl compound is first characterised in 1990 [A. Pring *et al.* Am. Mineral. 75: 1421 (1990)].

“…named in recognition of Glyn Francis’ contribution to the understanding and preservation of the minerals of the Iron Monarch ore body.” - A Pring *et al.* 1990

Francisite: $CuBi(SeO_3)_2O_2Cl$… or simply CBSCl

Single crystal samples

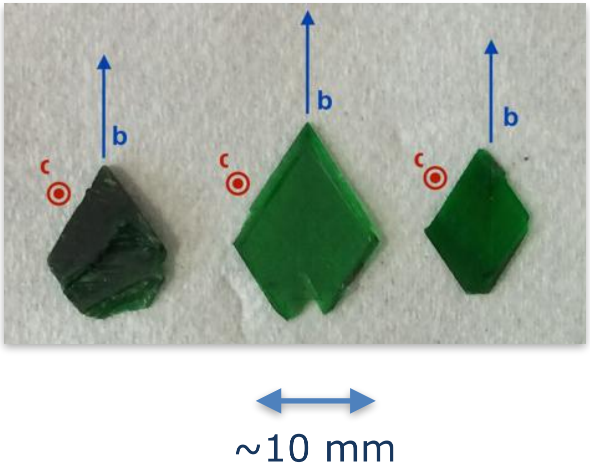

$Cu_3Bi(SeO_3)_2O_2Cl$

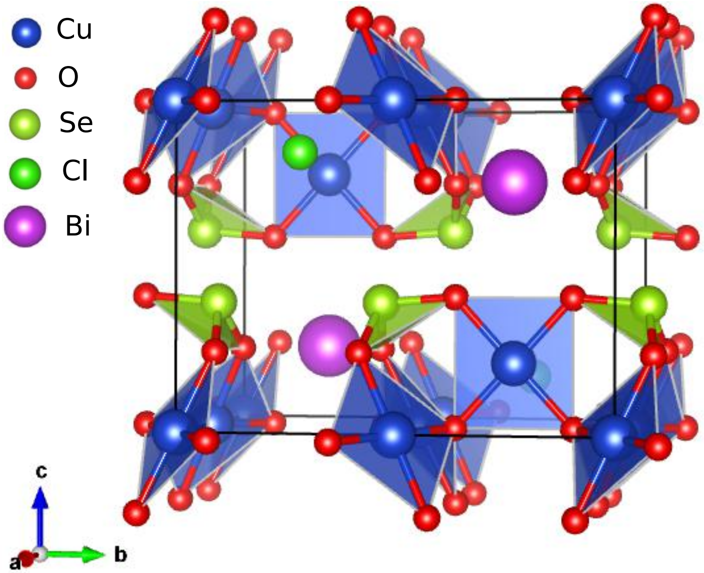

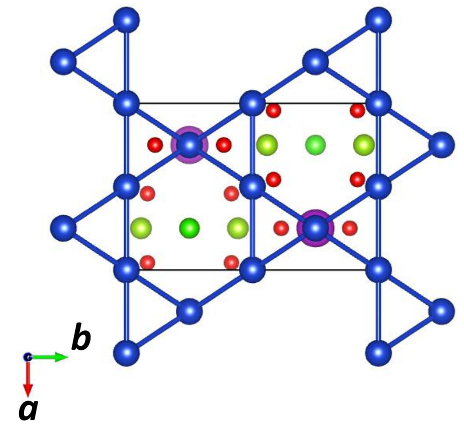

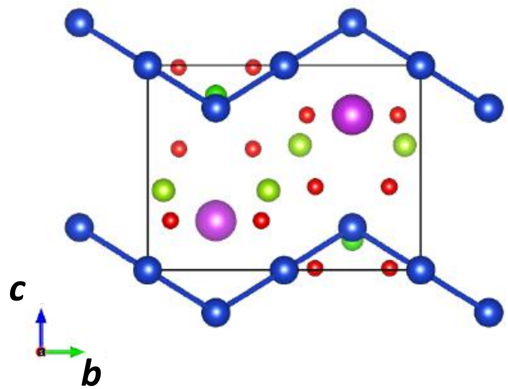

- Orthorhombic ***Pmmn*** space group (centrosymmetric).
  [A. Pring *et al.* Am. Mineral 1990]

- CuO_4 square plackets produce **buckled Cu^{2+} kagome lattice** layered along *c*.

- Layers are separated by SeO_3 triangular pyramids and Bi atoms.

- Cl atoms confined within centres of hexagonal tunnels.

Francisite: $CuBi(SeO_3)_2O_2Cl$… or simply CBSCl

Single crystal samples

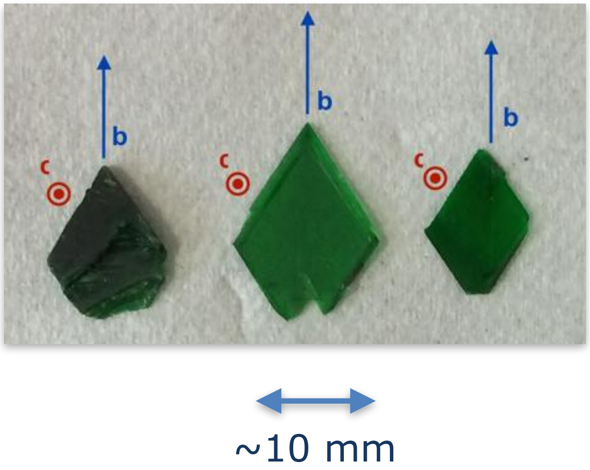

$Cu_3Bi(SeO_3)_2O_2Cl$

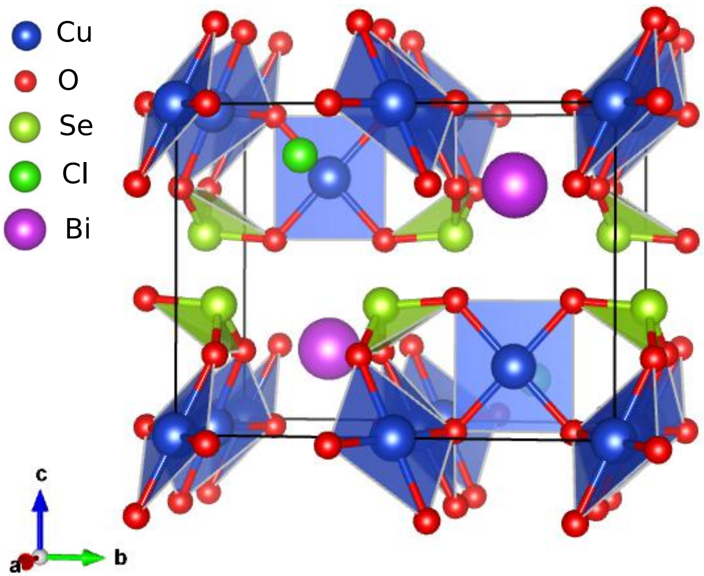

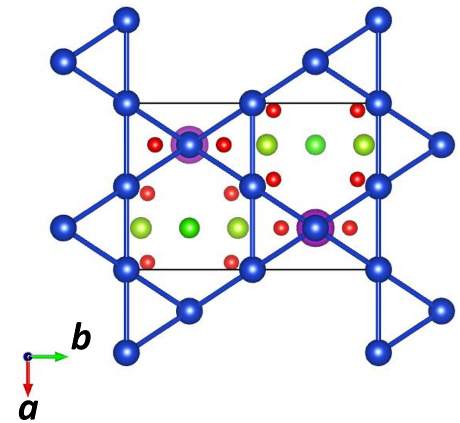

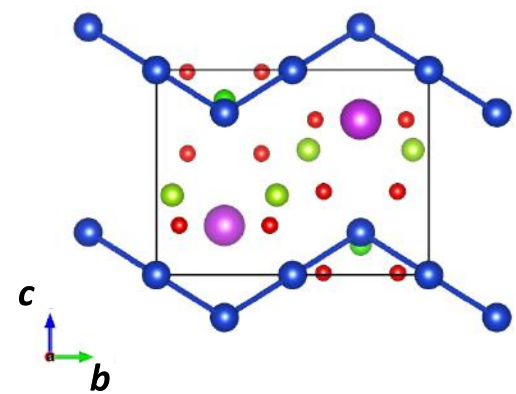

$CuBi(SeO_3)_2O_2$**X**; **X = Cl, Br, I**

$CuBi(SeO_3)_2O_2$**Br** **(CBSBr)**
$CuBi(SeO_3)_2O_2$**I** **(CBSI)**

Cu**Y**$(SeO_3)_2O_2Cl$
Cu**Sm**$(SeO_3)_2O_2Cl$
Cu**Er**$(SeO_3)_2O_2Cl$

Magnetic and dielectric interest

Magnetic frustration/order

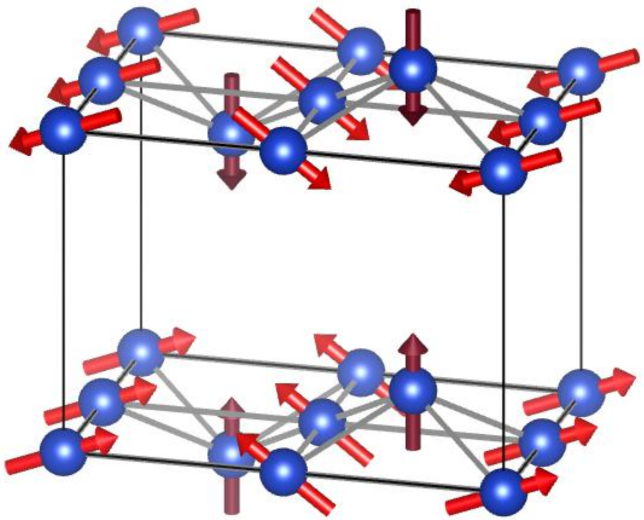

Magnetic susceptibility

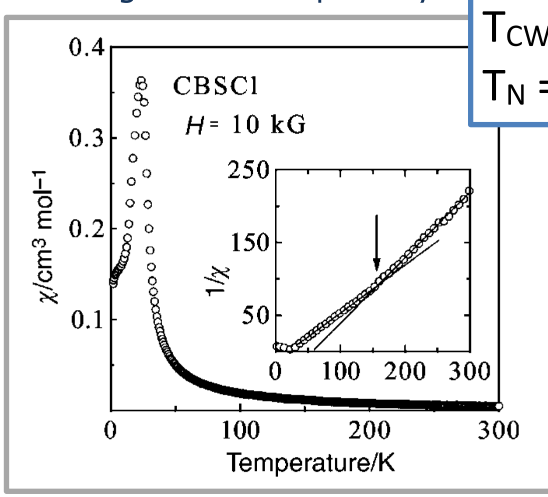

T_{CW} = +50K
T_N = 25K

Millet J. Mater. Chem. 11 (2001)

Antipolar distortion

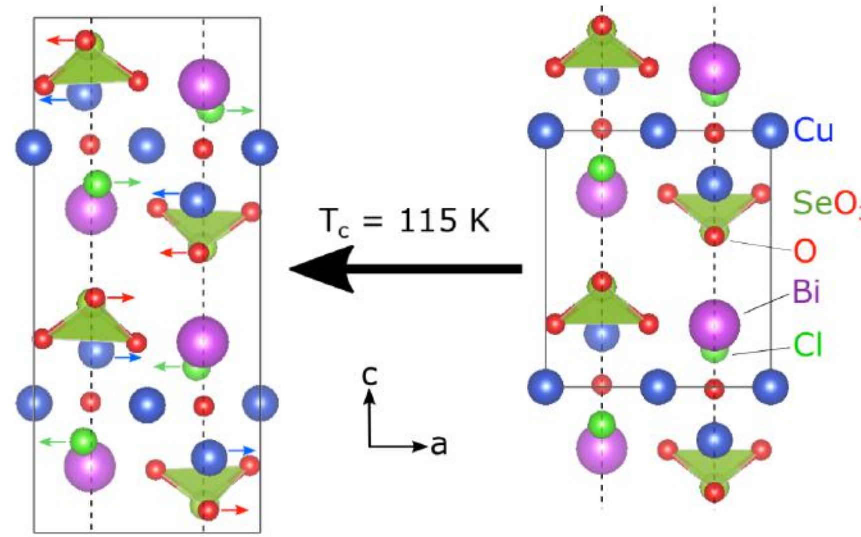

Pcmn ***Pmmn***

dielectric constant

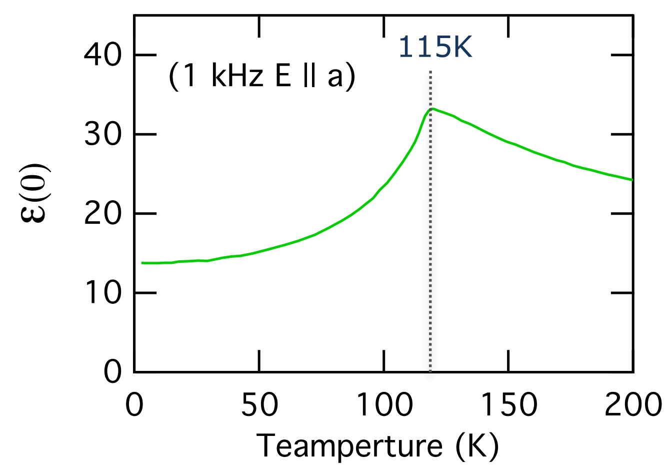

Antiferroelectrics: real or not?

Theory of Antiferroelectric Crystals

C. KITTEL
Department of Physics, University of California, Berkeley, California
(Received January 10, 1951)

effective field of each sub lattice

$$F_a = E + \beta_1 P_a - \beta_2 P_b; \quad F_b = E + \beta_1 P_b - \beta_2 P_a.$$

free energy

$$A(P_a, P_b, T) = A_0 + f(P_a^2 + P_b^2) + g P_a P_b + h(P_a^4 + P_b^4).$$

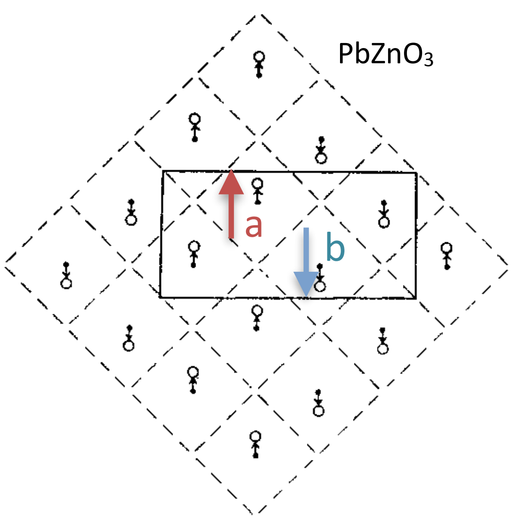

Sawaguchi Phys. Rev. **83** (1951)

Soft-mode spectroscopy: Experimental studies of structural phase transitions*

J. F. Scott
Department of Physics, University of Colorado, Boulder, Colorado 80302
Reviews of Modern Physics, Vol. 46, No. 1, January 1974

"…in general one cannot characterize a crystal at one temperature as antiferroelectric by any set of experimental measurements at that temperature."

"…antiferroelectricity is an ill defined, almost useless concept."

$P_{total} = 0$

How do you define a sub lattice polarisation?

No macroscopic order parameter

No broken symmetries!

PHYSICAL REVIEW B **94**, 014107 (2016)

Theory of antiferroelectric phase transitions

Pierre Tolédano[1] and Mael Guennou[2,*]
[1]*Laboratoire de Physique des Systèmes Complexes, Université de Picardie, 80000 Amiens, France*
[2]*Materials Research and Technology Department, Luxembourg Institute of Science and Technology, 41 rue du Brill, L-4422 Belvaux, Luxembourg*
(Received 20 January 2016; revised manuscript received 6 May 2016; published 11 July 2016)

$$\phi(\eta, P, T) = \phi_0(T) + \frac{\alpha}{2}\eta^2 + \frac{\beta}{4}\eta^4 + \frac{\gamma}{6}\eta^6 + \frac{P^2}{2\chi_0} + \frac{\delta}{2}\eta^2 P^2 - EP,$$

- local polar point group symmetry as order parameter.
- Displacive AFE characterised by **soft antipolar phonon mode**

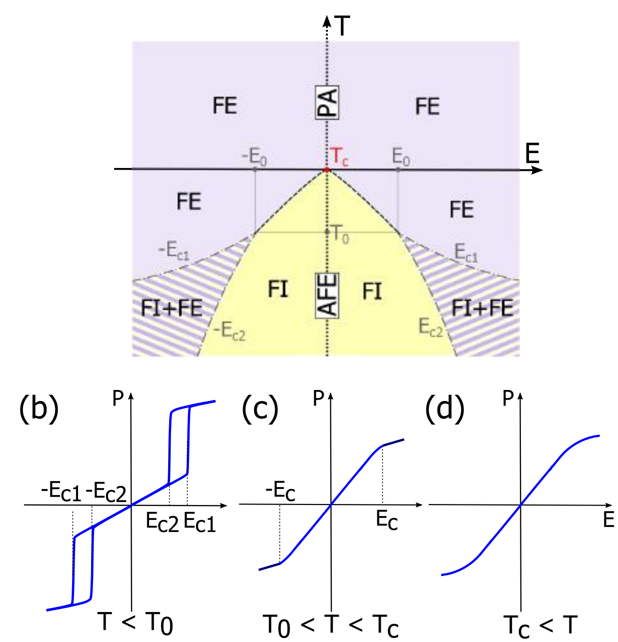

Antiferroelectric signatures

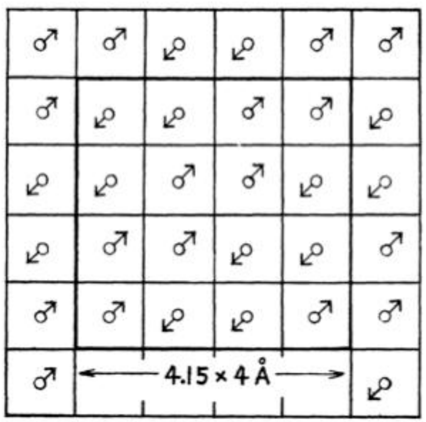

Fig. 11. A model of the atomic arrangement of $PbZrO_3$, (001) plane. Although the true symmetry may be orthorhombic, we choose here tetragonal axes. An arrow shows the displacement of a heavy ion (probably a Pb ion).

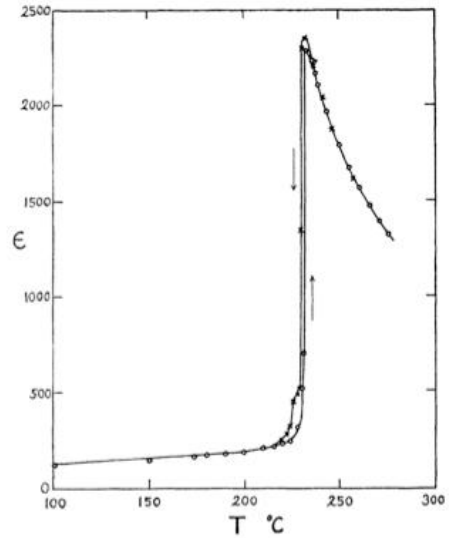

Fig. 2. Dielectric constant of lead zirconate at varying temperatures.

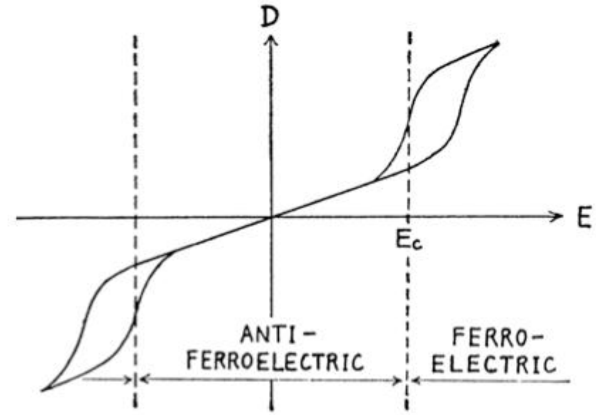

Tentative explanation of the anomalous hysteresis loops of $PbZrO_3$ at 30 kv/cm.

- Antipolar atomic displacements
- Phase transition between two non-polar phases
- Dielectric anomaly at the transition
- Polar phase induced by electric field

Uses

- Energy storage
- Electrocalorics
- Large strain actuators
- (Multistate) memories

Issues

- Ambiguities of the double loop.
- What is a sublattice polarisation ?
- Absence of a symmetry criterion.
- Antiferroelectricity in PbZrO3 is a complex model.

Lattice contribution to dielectric response along **a**

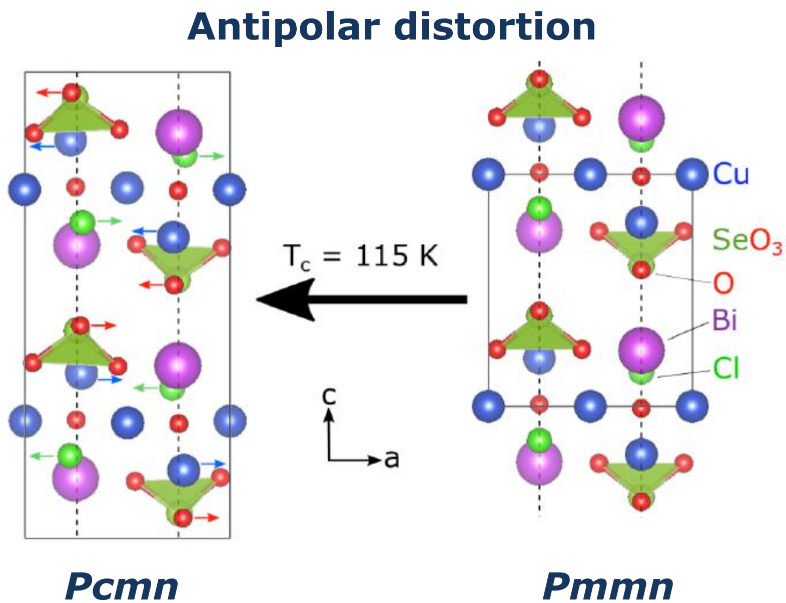

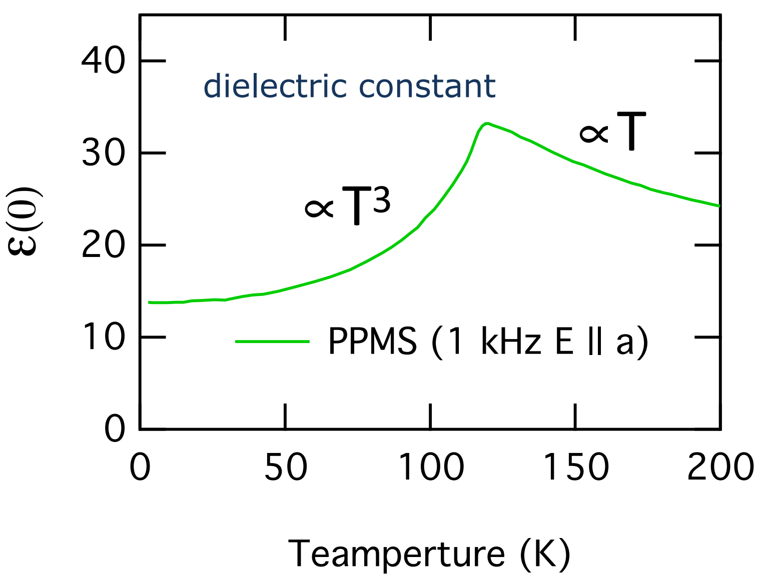

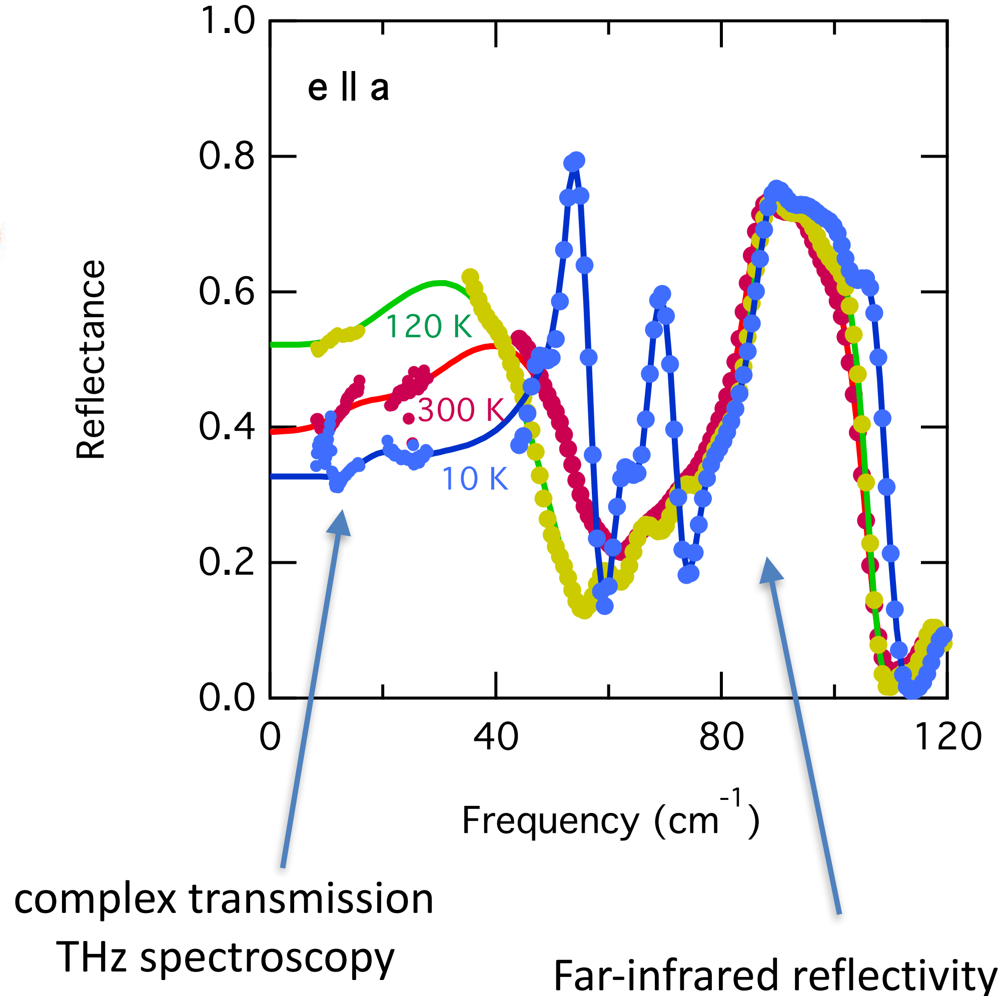

Lattice contribution to dielectric response along **a**

Kramers-Kronig transform

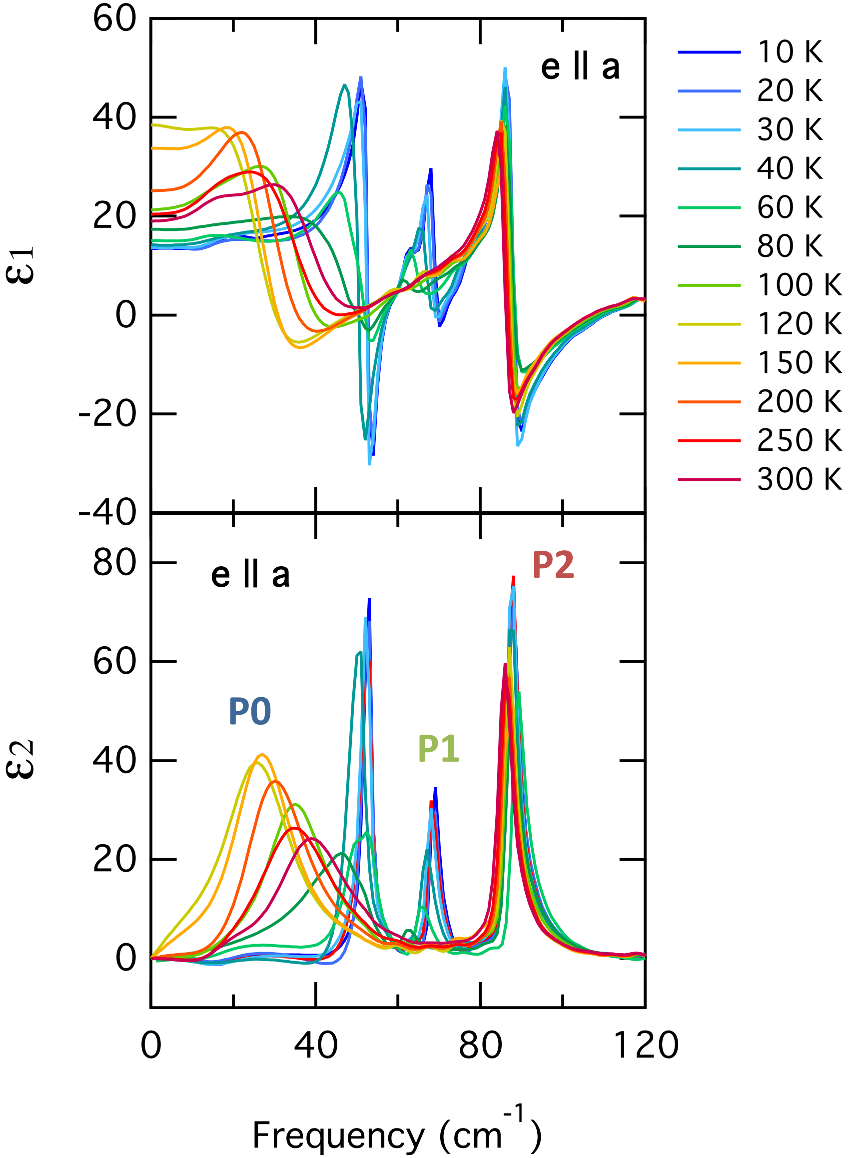

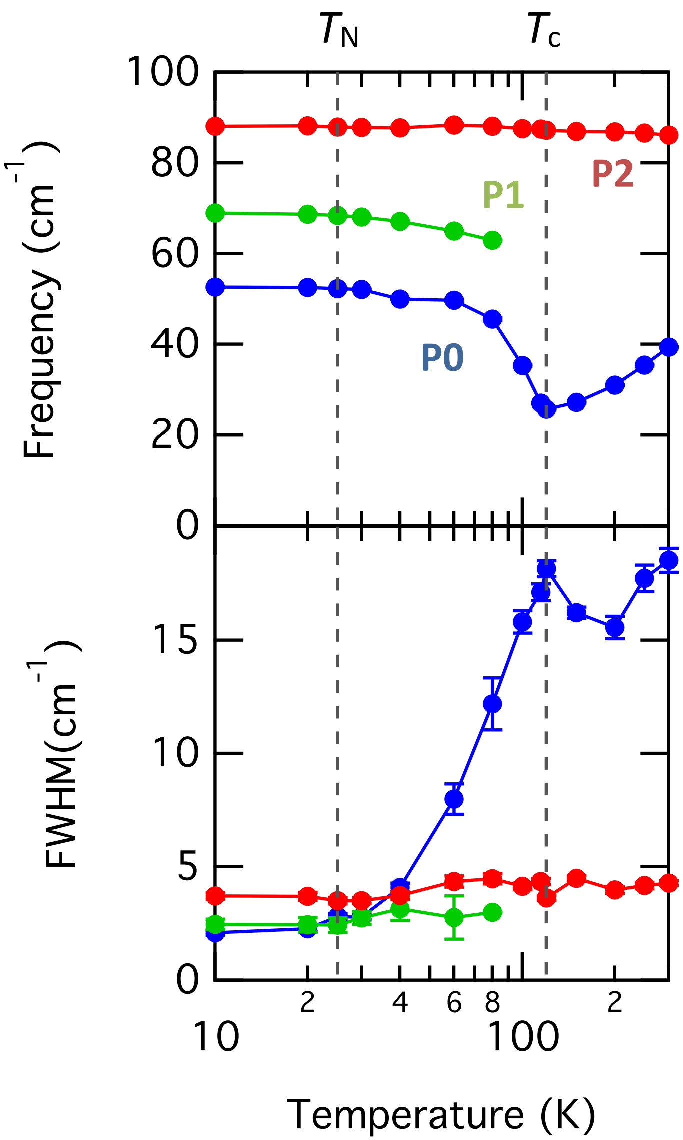

Lattice contribution to dielectric response along **a**

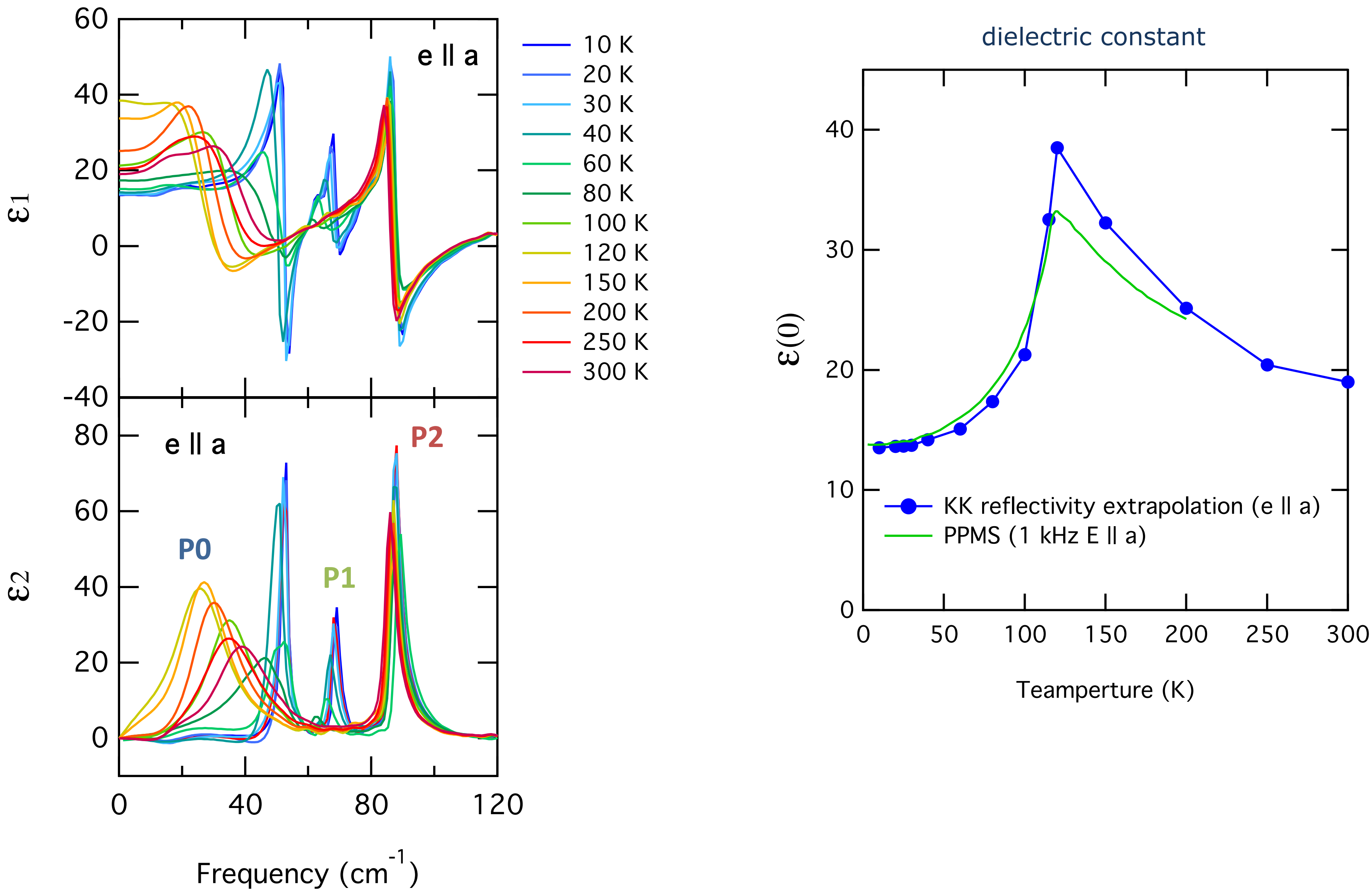

Dielectric response of soft antipolar mode

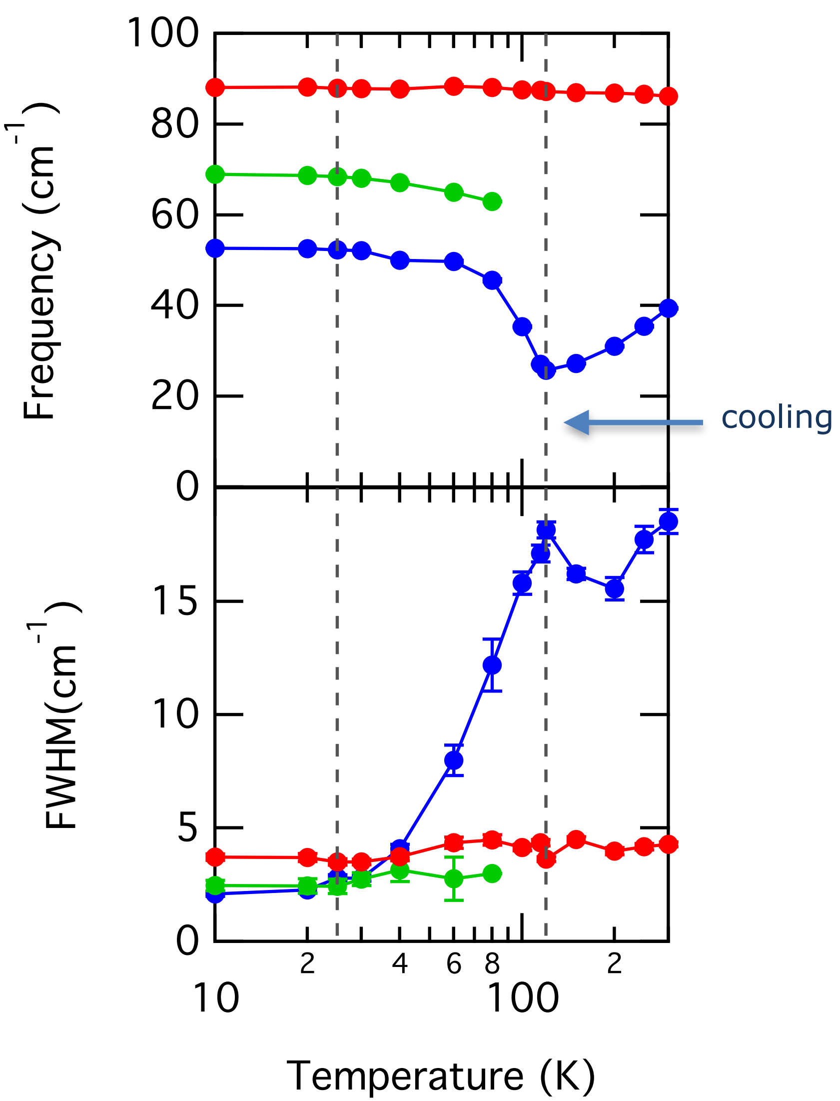

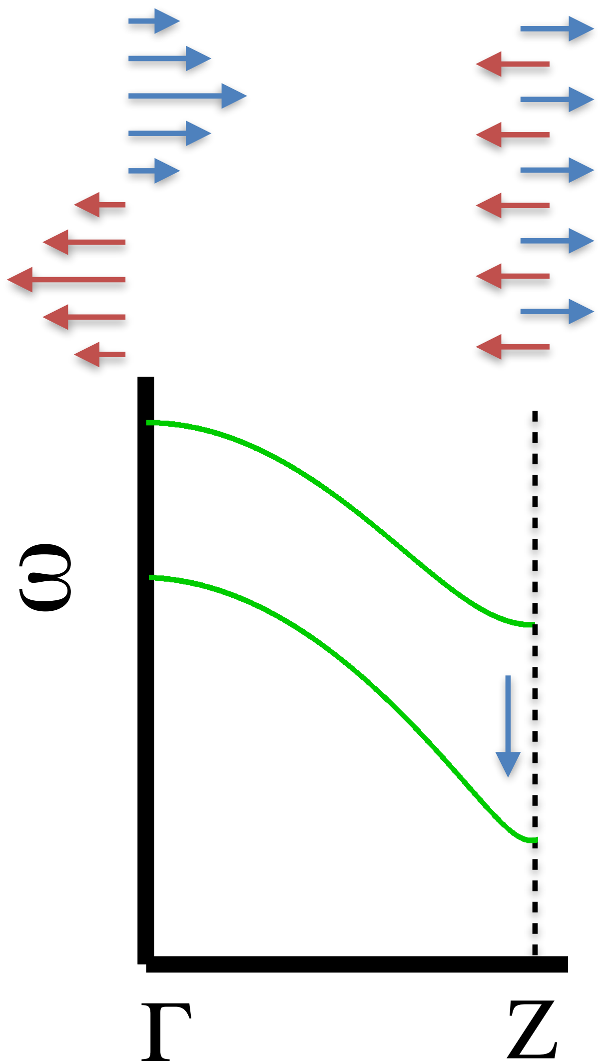

Dielectric response of soft antipolar mode

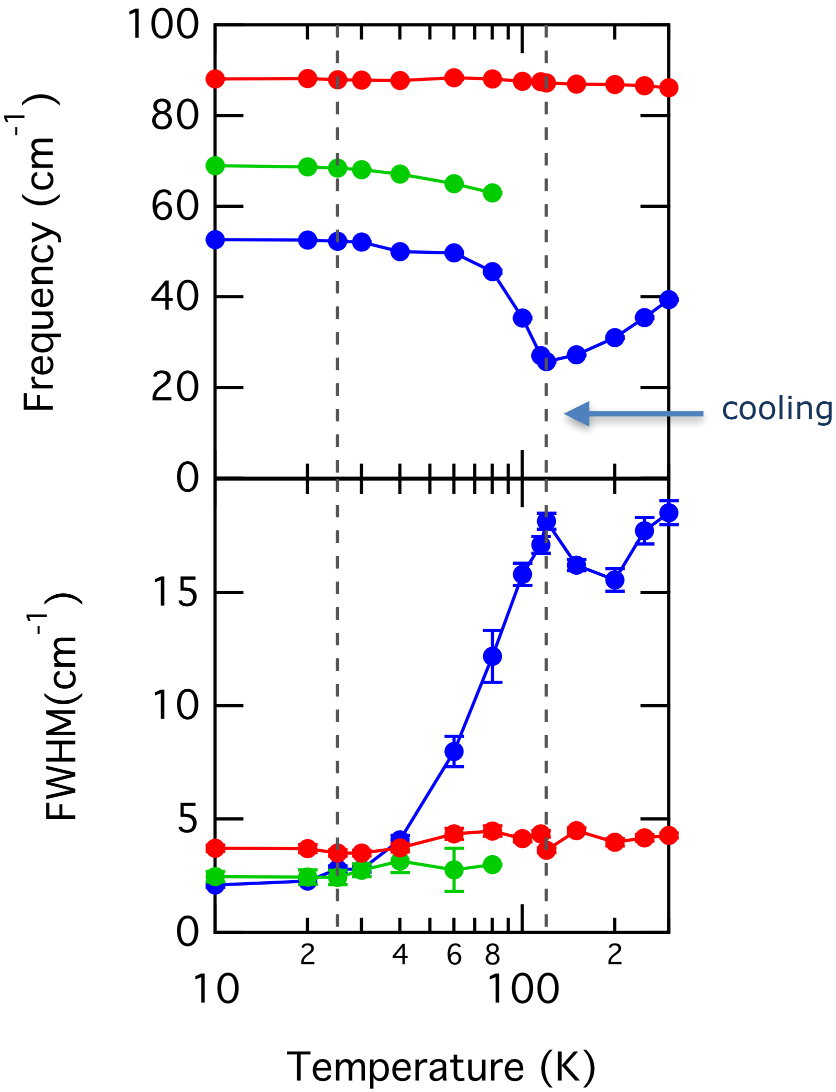

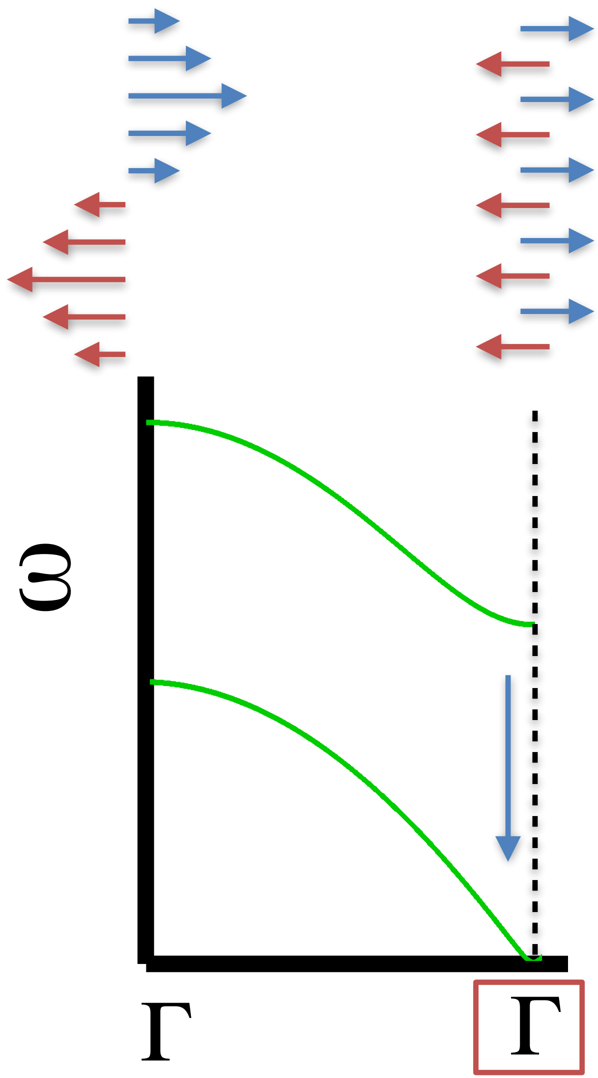

Dielectric response of soft antipolar mode

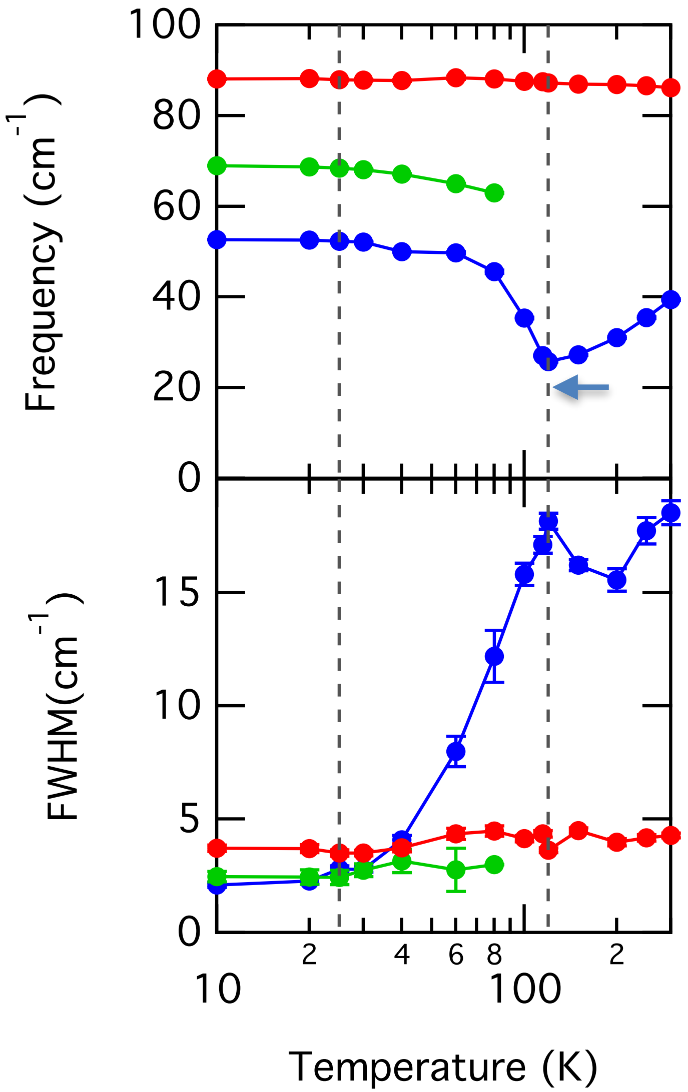

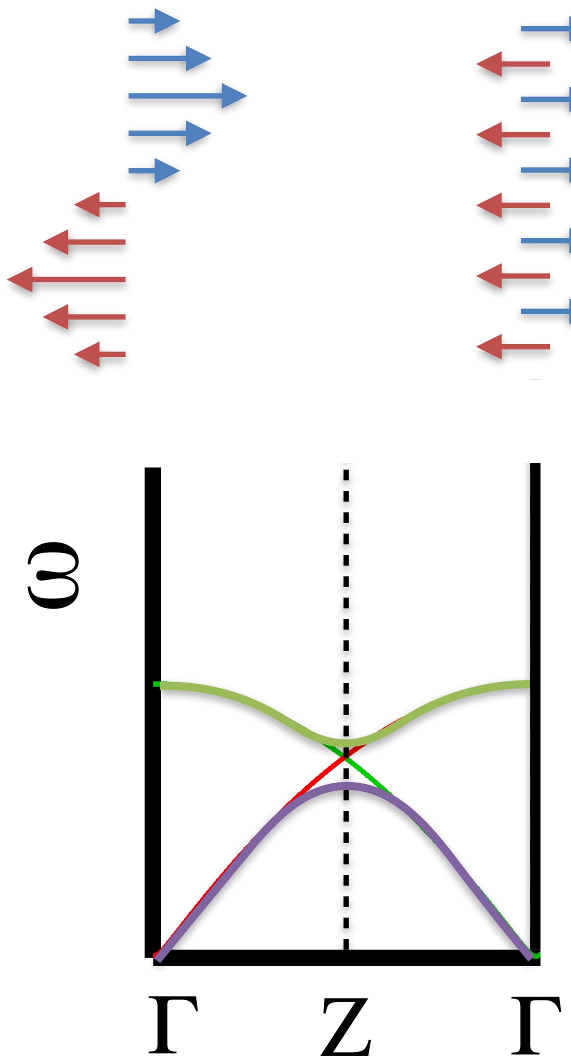

Unit cell doubling

Dielectric response of soft antipolar mode

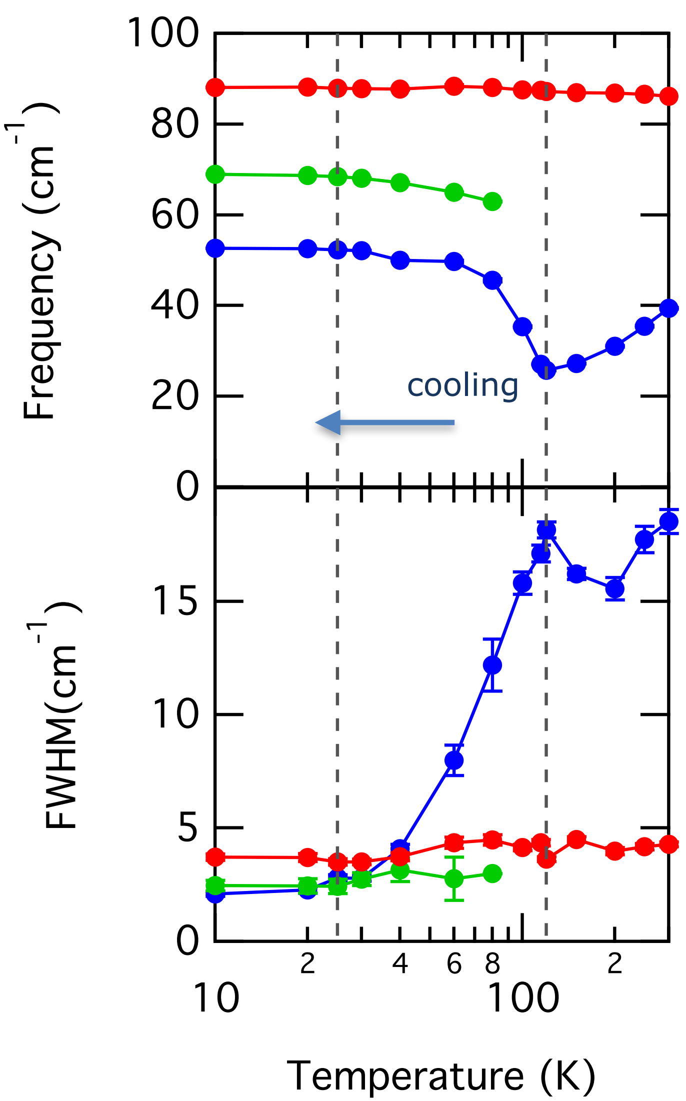

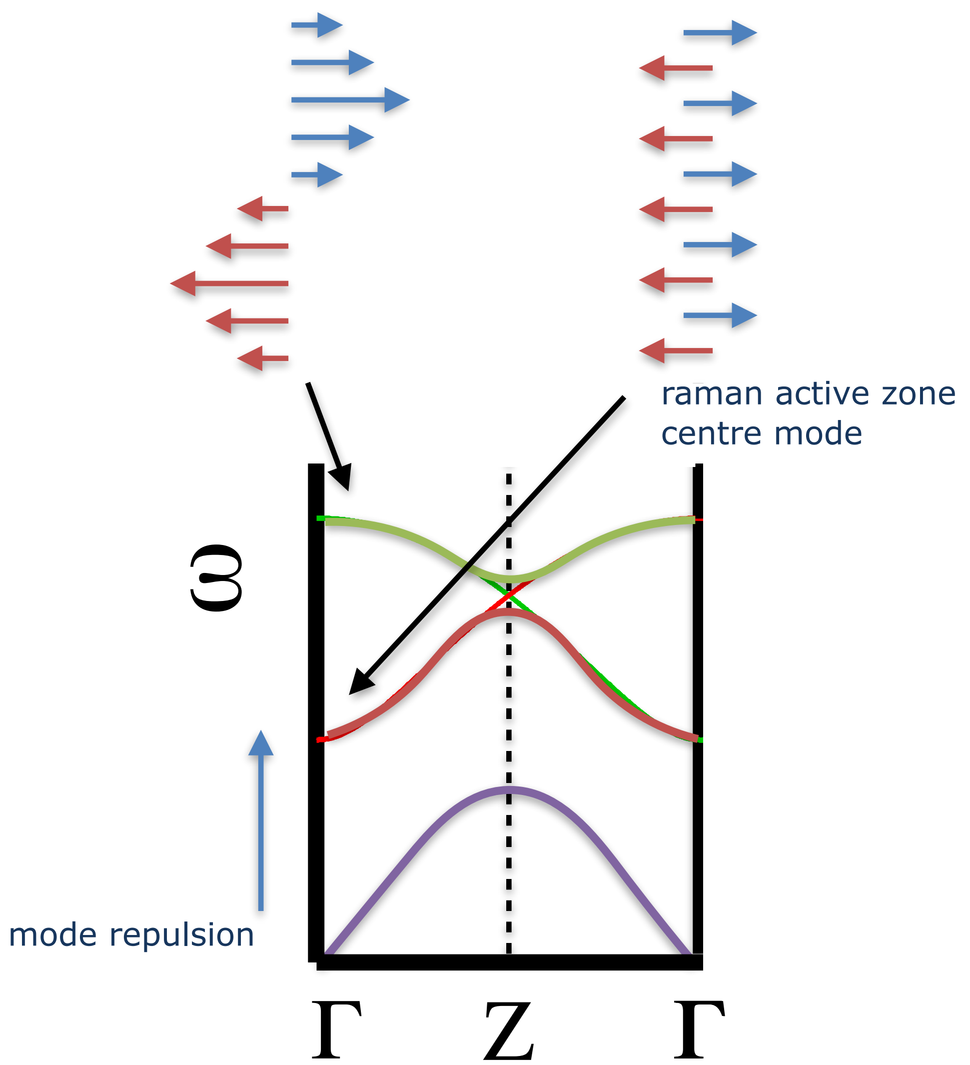

Raman phonon dynamics

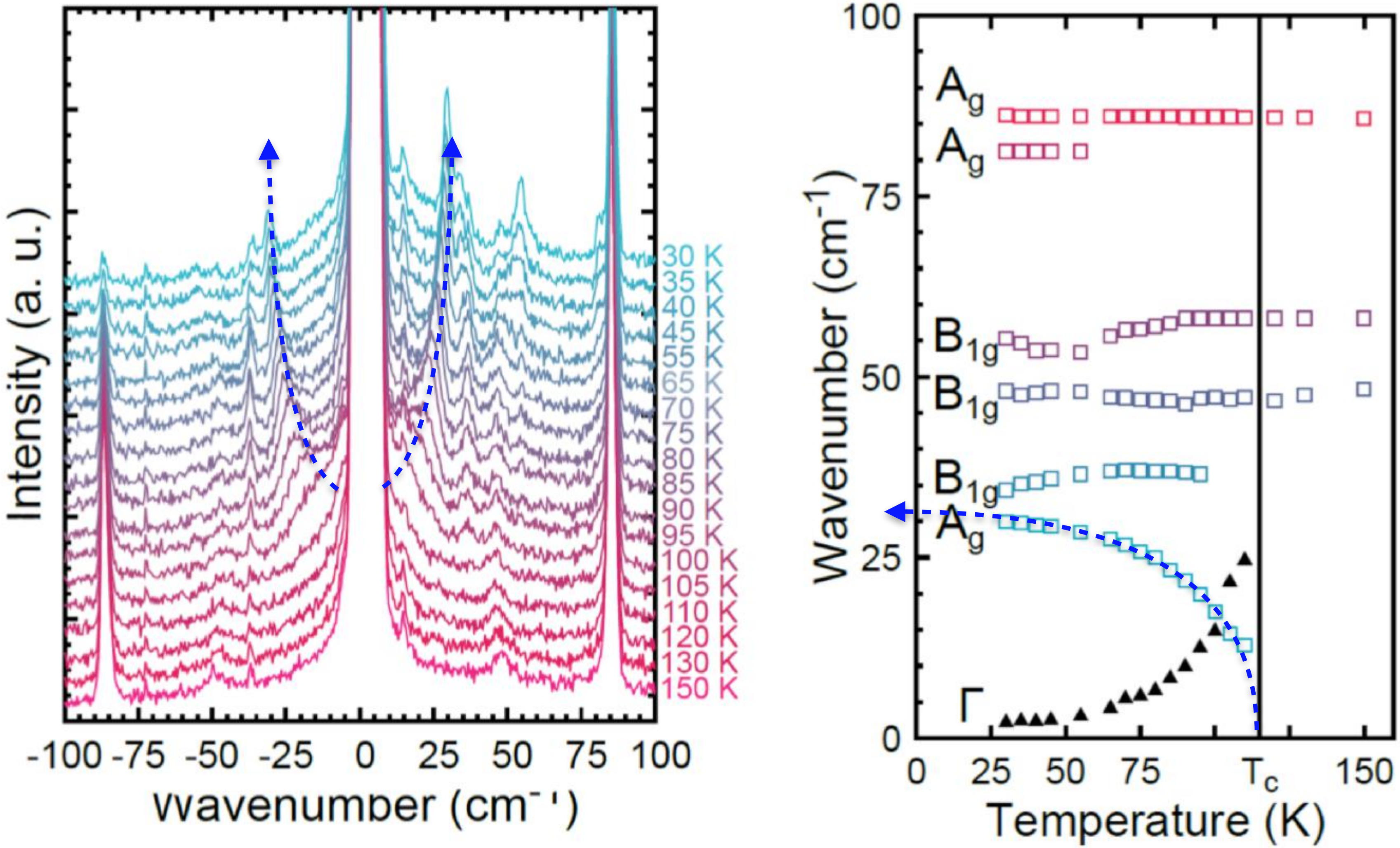

Inelastic xray scattering soft mode dispersion

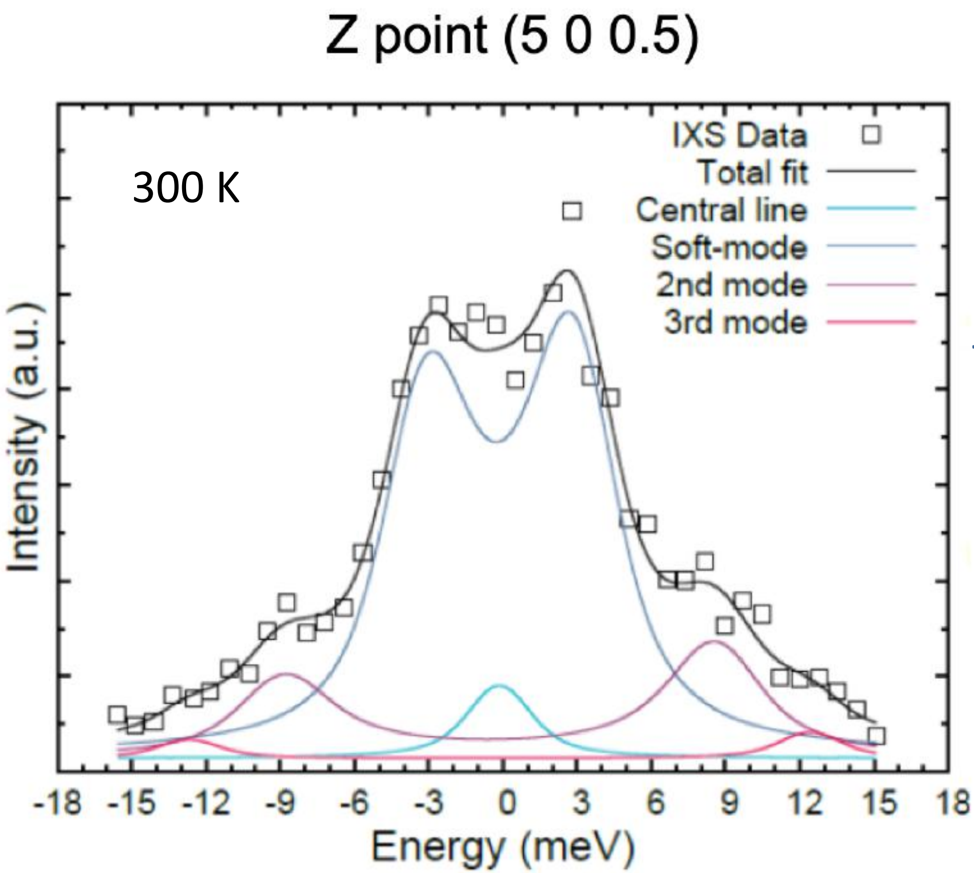

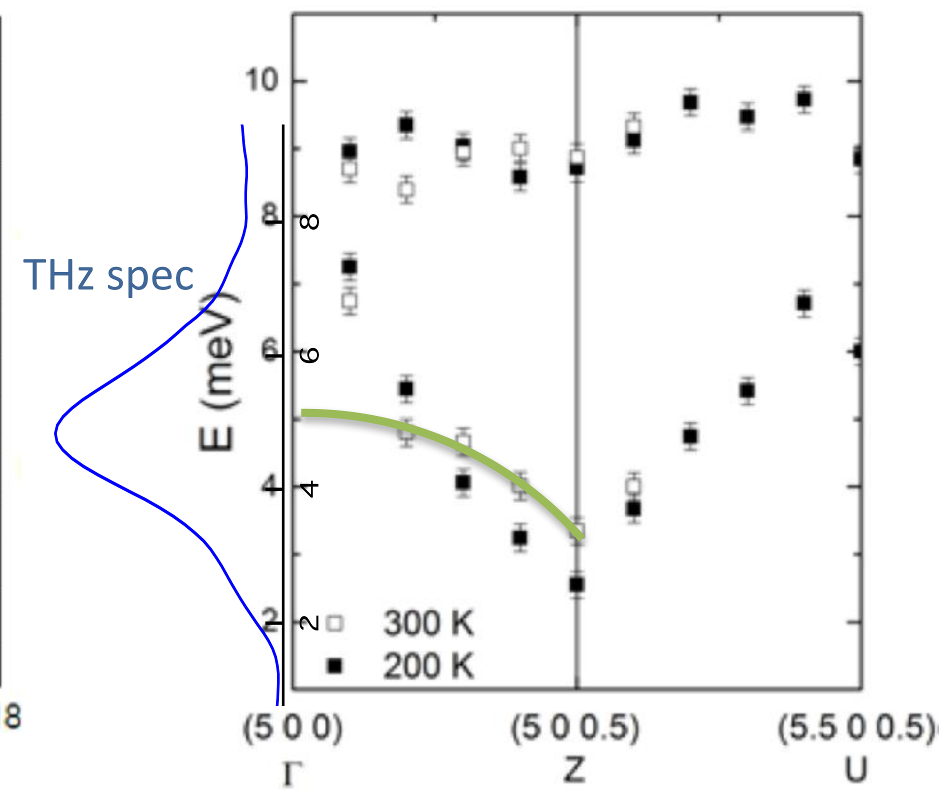

Inelastic Xray scattering soft mode dynamics

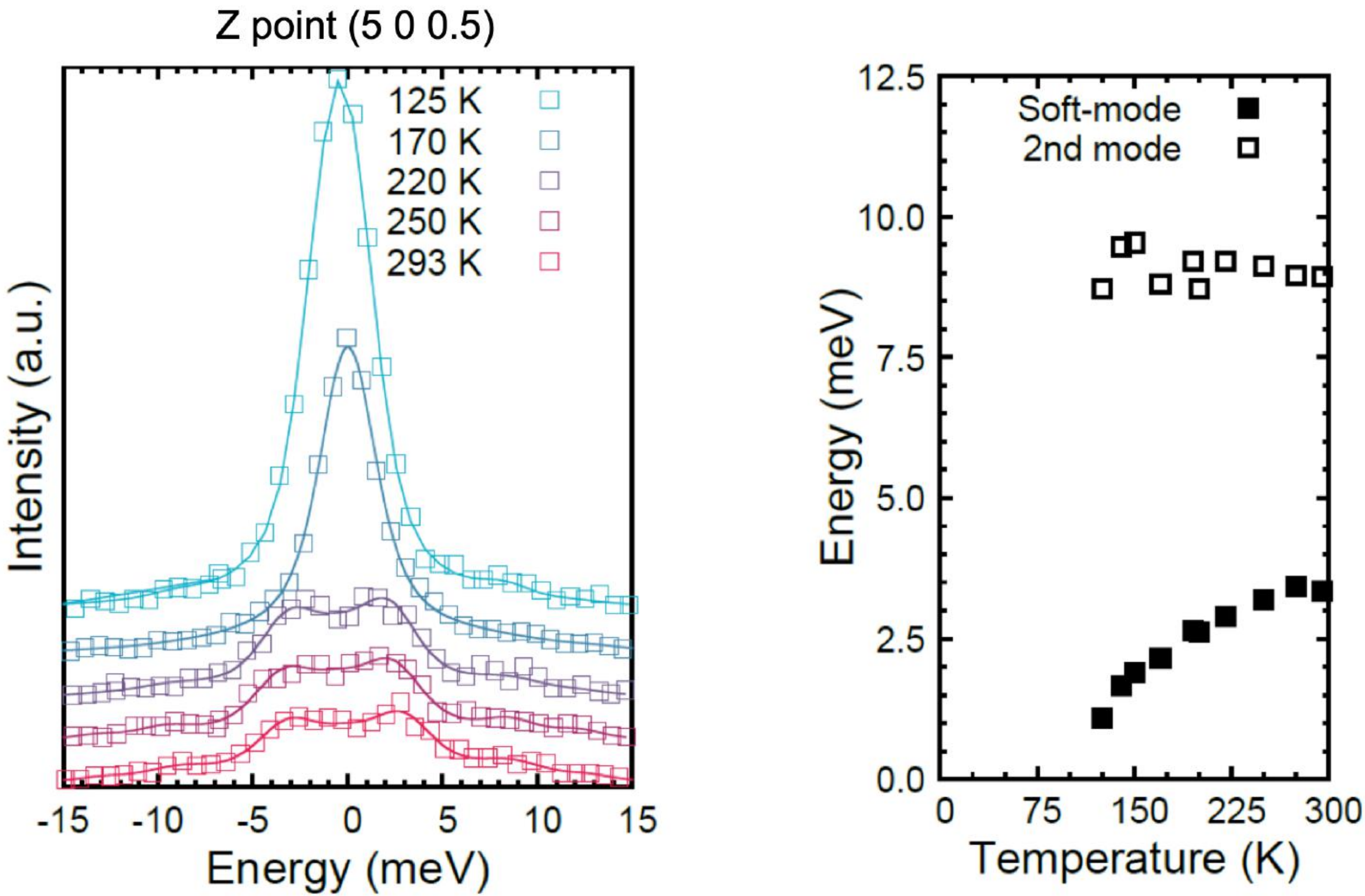

Elastic Thermal Diffuse Xray Scattering (TDS)

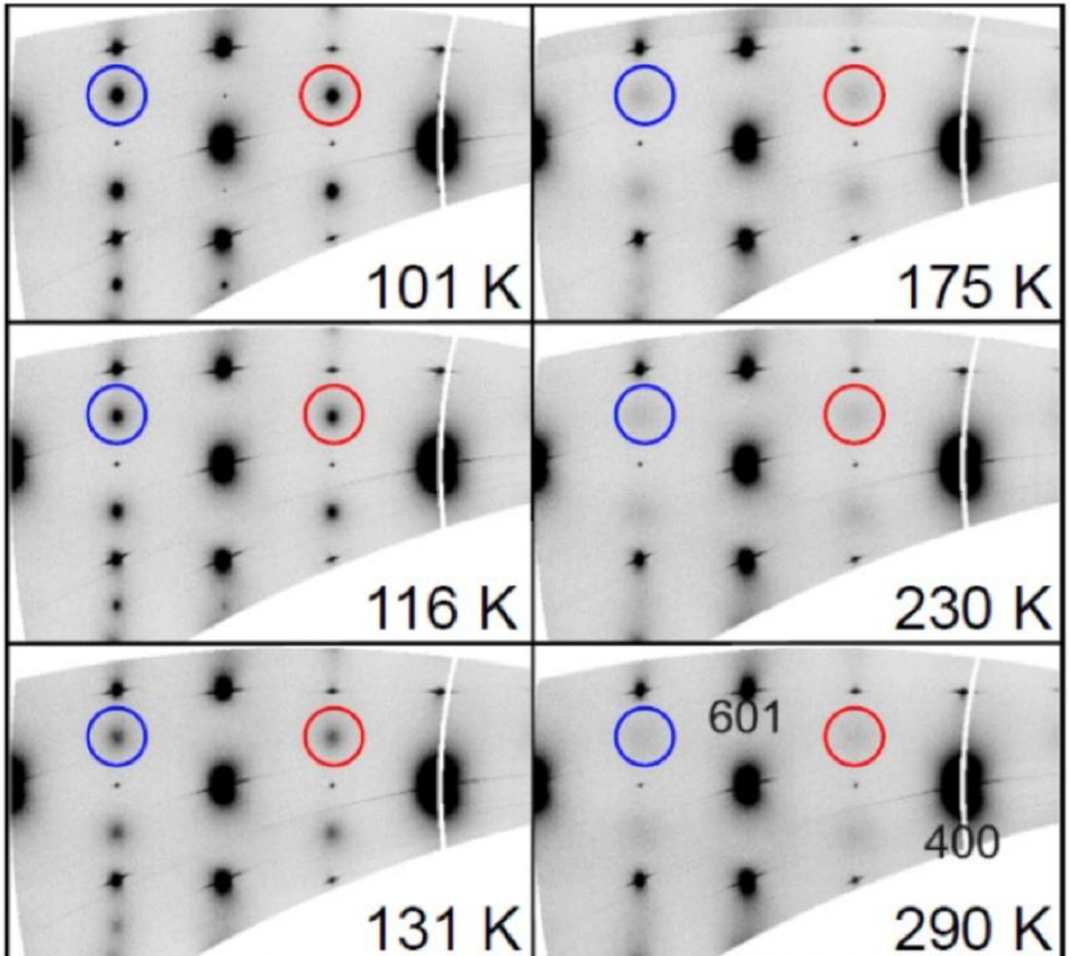

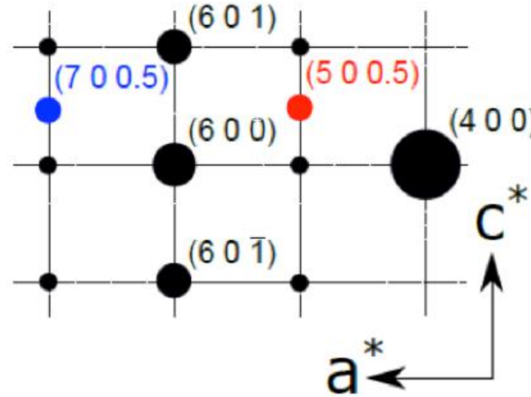

$$I_{\mathrm{TDS}}(\vec{Q}) \approx \frac{1}{\omega(\vec{q})} \coth\left(\frac{\hbar\omega(\vec{q})}{2k_{\mathrm{B}}T}\right) f(\vec{Q})^2$$

Soft-mode frequency

Elastic Thermal Diffuse Xray Scattering (TDS)

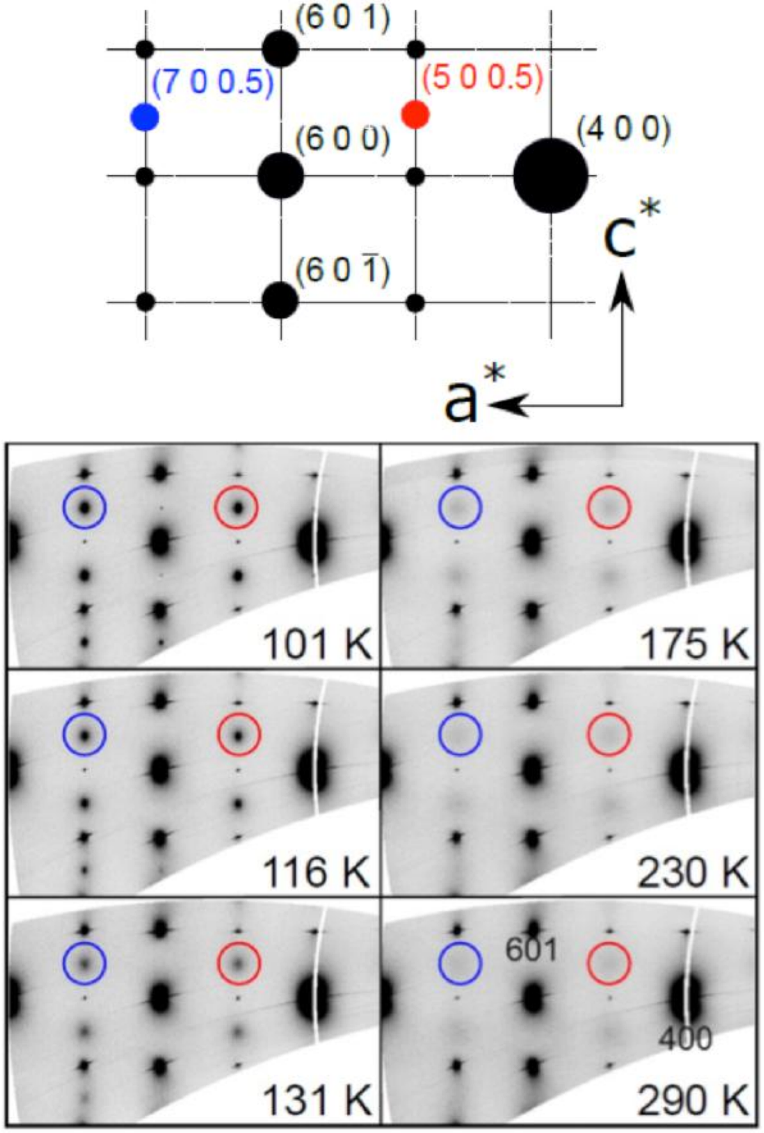

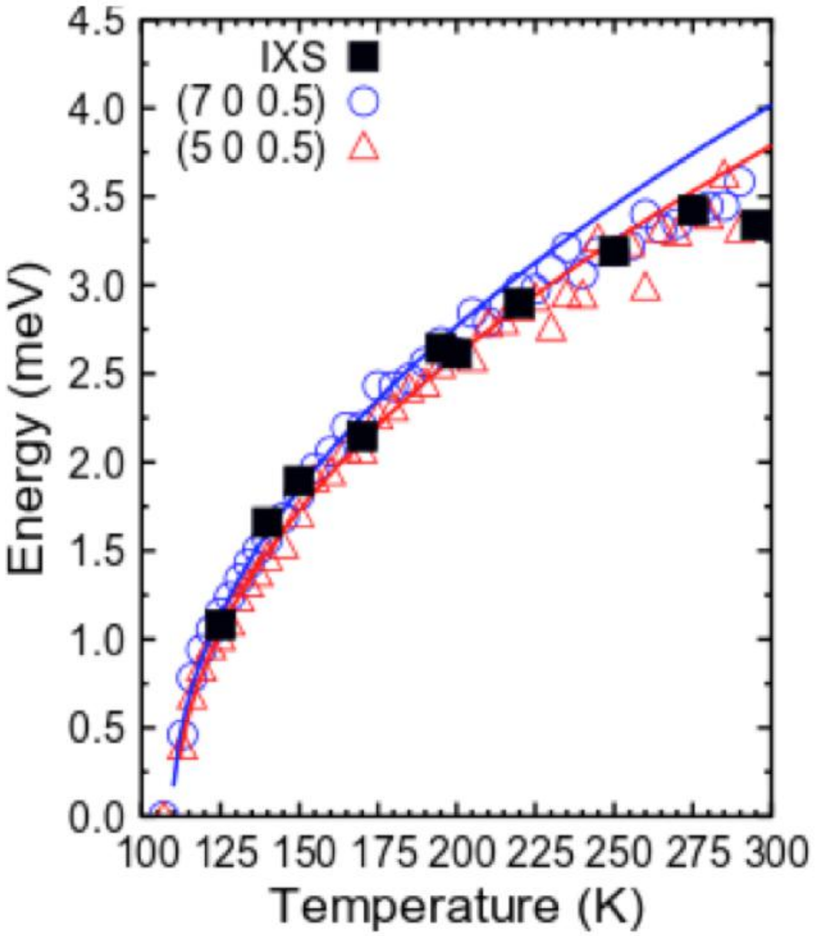

Antipolar softmode dynamics

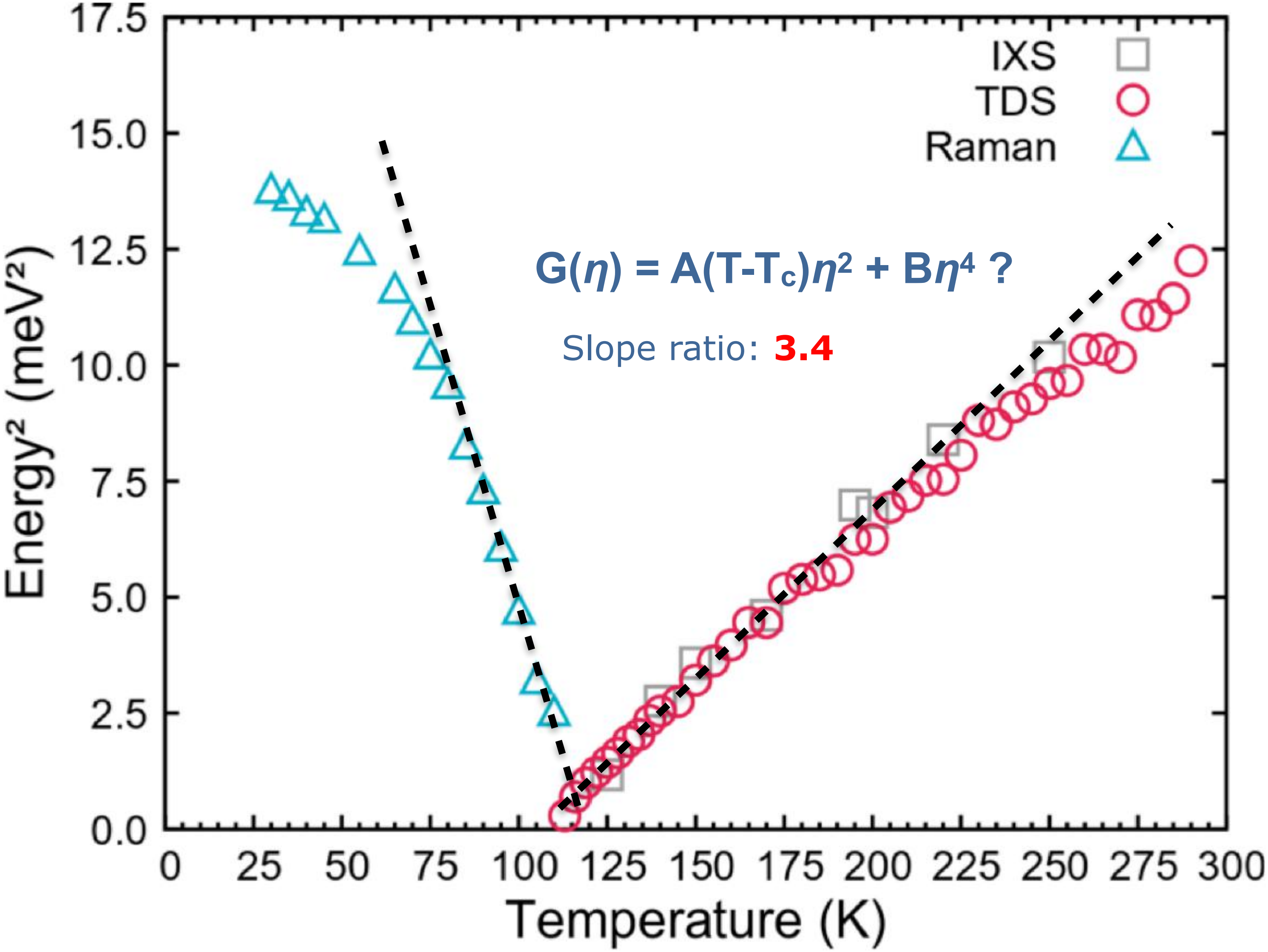

Antipolar softmode dynamics

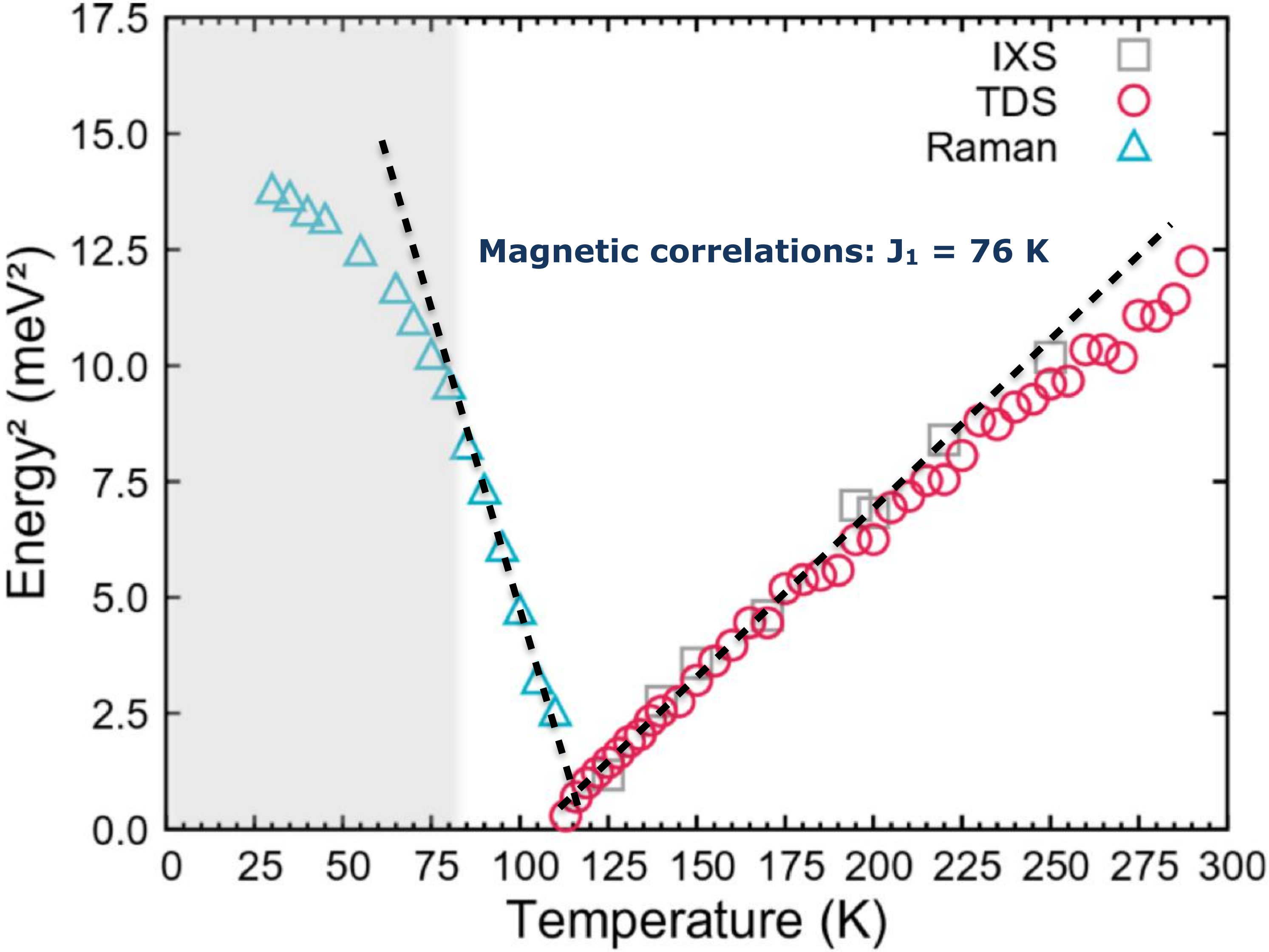

Magnetic structure: k = (0, 0, 1/2) antiferromagnet

Two S = 1/2 Cu^{2+} sites: Cu1 at (0,0,0) 4c and Cu2 at (1/4, 1/4, z) 2c.

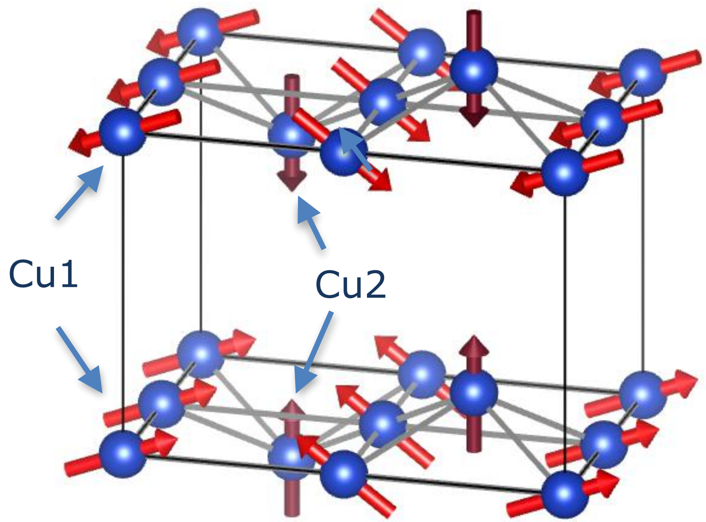

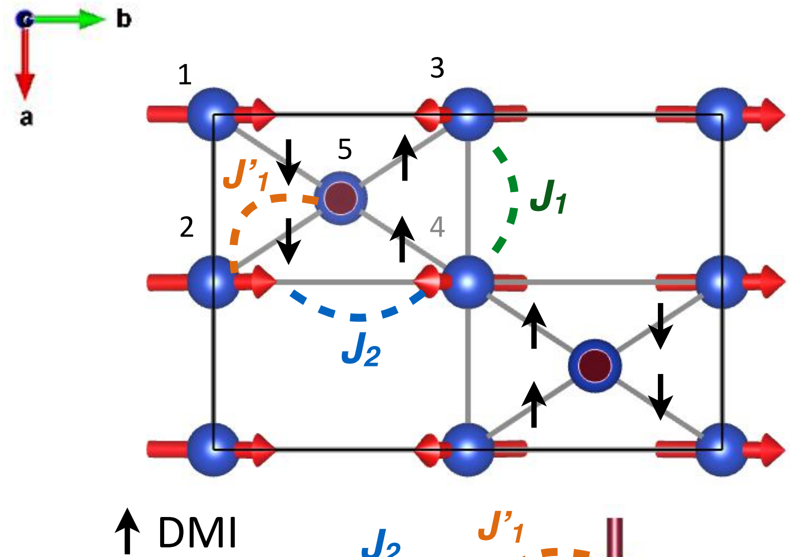

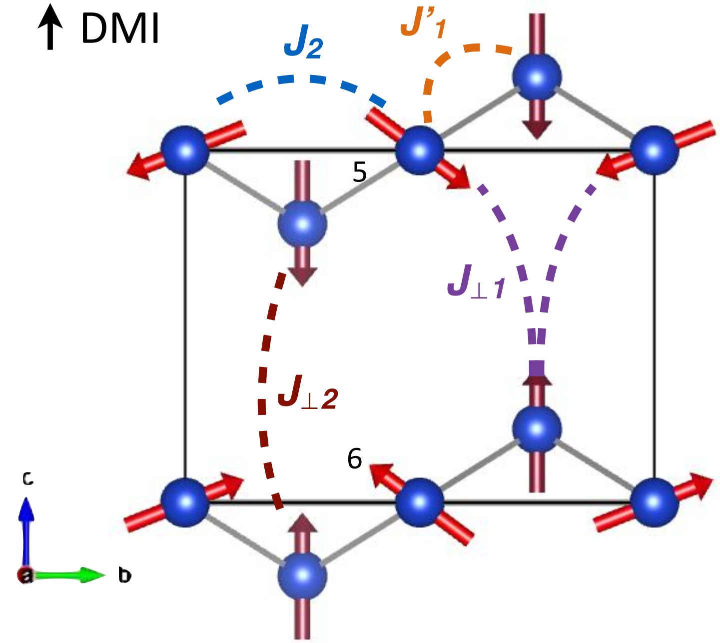

$$H = J_1 \sum_{\substack{i=1,3\\ j=2,4}} \boldsymbol{S_i} \cdot \boldsymbol{S_j} + J_1' \sum_{\substack{i=1-4\\ j=5}} \boldsymbol{S_i} \cdot \boldsymbol{S_j} + J_2 \sum_{\substack{i=1,2\\ j=3,4}} \boldsymbol{S_i} \cdot \boldsymbol{S_j}$$

$$+ J_{\perp 1} \sum_{\substack{i=1-4\\ j=6}} \boldsymbol{S_i} \cdot \boldsymbol{S_j} + J_{\perp 2} \sum_{\substack{i=5\\ j=6}} \boldsymbol{S_i} \cdot \boldsymbol{S_j} + \boldsymbol{D} \cdot \sum_{\substack{i=1-4\\ j=5}} \boldsymbol{S_i} \times \boldsymbol{S_j},$$

Context of magnetic research interest

S = 1/2 antiferromagnetic kagome lattice is the archetype of quantum spin liquids.

Francisite represents **kagome system beyond nearest neighbour antiferromagnets:**

- Nearest neighbour ferromagnetic interactions.
- Competing antiferromagnetic interactions across hexagonal voids.

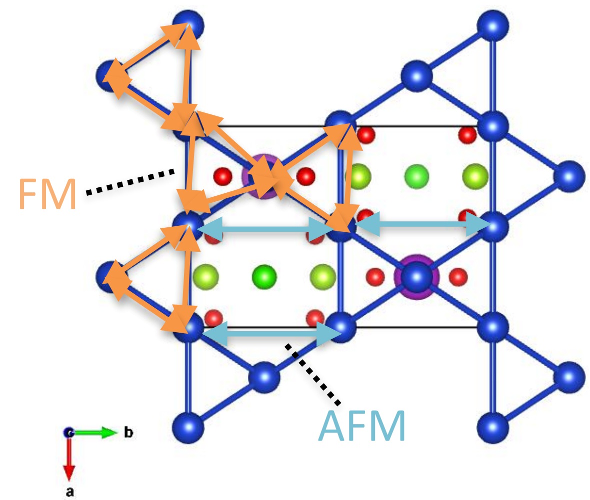

May support novel phases:

- Non-coplanar spin correlation and spin liquid states
  - e.g. Kapellasite [B. Fåk PRL 2012]
- magnetically induced ferroelectricity:
  - e.g. multiferroic $KCi_3As_2O_7(OD)_3$ [G. L. Nilsen PRB(R) 2014]

Q = (0 k 2) map comparison with simulation

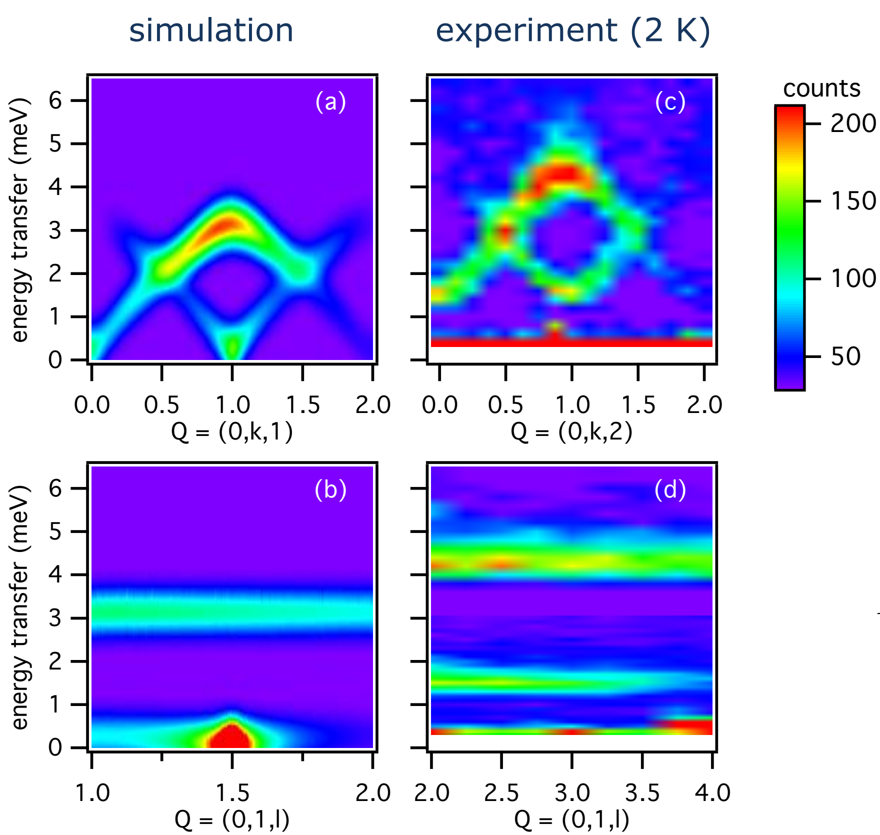

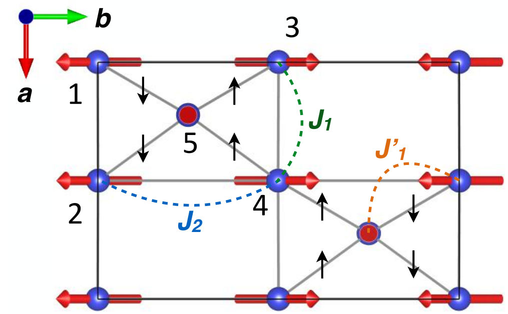

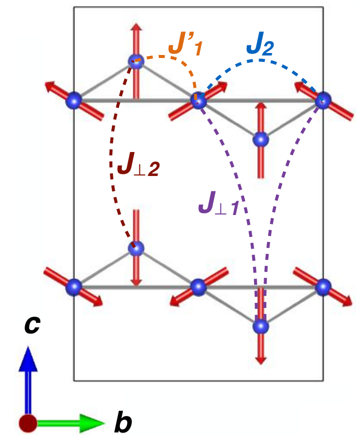

J_1 = -6.55 meV J'_1 = -5.75 meV

$J_{\perp 1}$ = 0.035 meV $J_{\perp 2}$ = 0.17 meV

J_2 = 4.9 meV D_x = 1.04 meV

$$H = J_1 \sum_{\substack{i=1,3\\ j=2,4}} \boldsymbol{S_i} \cdot \boldsymbol{S_j} + J'_1 \sum_{\substack{i=1-4\\ j=5}} \boldsymbol{S_i} \cdot \boldsymbol{S_j} + J_2 \sum_{\substack{i=1,2\\ j=3,4}} \boldsymbol{S_i} \cdot \boldsymbol{S_j}$$
$$+ J_{\perp 1} \sum_{\substack{i=1-4\\ j=6}} \boldsymbol{S_i} \cdot \boldsymbol{S_j} + J_{\perp 2} \sum_{\substack{i=5\\ j=6}} \boldsymbol{S_i} \cdot \boldsymbol{S_j} + \boldsymbol{D} \cdot \sum_{\substack{i=1-4\\ j=5}} \boldsymbol{S_i} \times \boldsymbol{S_j}$$

- Dispersion shape and extinction along *k* reproduced well in simulations using proposed Hamiltonian.
- No dispersion along *l* confirms very weak interlayer coupling and “global” spin gap.
- **Simulation does not reproduce spin gap.**

Modification with anisotropic exchange interaction

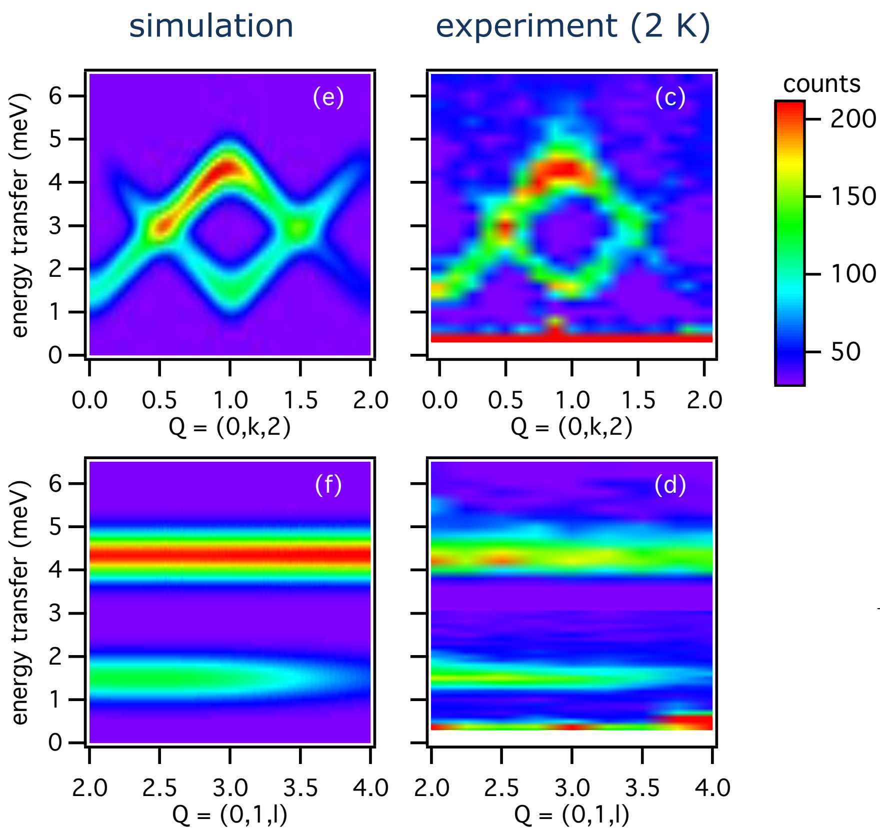

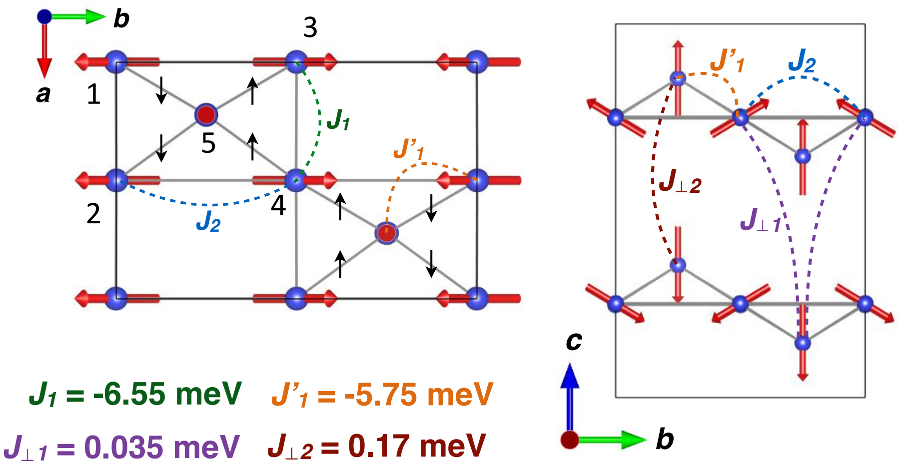

$J_1 = -6.55$ meV $J'_1 = -5.75$ meV

$J_{\perp 1} = 0.035$ meV $J_{\perp 2} = 0.17$ meV

$J_2 = 4.9$ meV $D_x = 1.04$ meV

$$H = J_1 \sum_{\substack{i=1,3\\ j=2,4}} \boldsymbol{S_i}\cdot\boldsymbol{S_j} + J_1' \sum_{\substack{i=1-4\\ j=5}} \boldsymbol{S_i}\cdot\boldsymbol{S_j} + J_2 \sum_{\substack{i=1,2\\ j=3,4}} \boldsymbol{S_i}\cdot\boldsymbol{S_j}$$

$$+ J_{\perp 1} \sum_{\substack{i=1-4\\ j=6}} \boldsymbol{S_i}\cdot\boldsymbol{S_j} + J_{\perp 2} \sum_{\substack{i=5\\ j=6}} \boldsymbol{S_i}\cdot\boldsymbol{S_j} + \boldsymbol{D}\cdot \sum_{\substack{i=1-4\\ j=5}} \boldsymbol{S_i}\times\boldsymbol{S_j}$$

$$+ \ \mathbf{S}_i \cdot \boldsymbol{\Gamma}_{i,j} \cdot \mathbf{S}_j,$$

$$\Gamma_{5,2} = \begin{pmatrix} \underline{0.10} & 0.08 & 0.00 \\ 0.08 & 0.00 & 0.04 \\ 0.00 & 0.04 & 0.00 \end{pmatrix},$$

$$\Gamma_{1,2} = \begin{pmatrix} 0.00 & 0.00 & 0.00 \\ 0.00 & 0.05 & \underline{0.12} \\ 0.00 & \underline{0.12} & 0.05 \end{pmatrix},$$

(in meV)

$$\Gamma_{4,2} = \begin{pmatrix} \underline{-0.7} & 0.0 & 0.0 \\ 0.0 & 0.0 & 0.0 \\ 0.0 & 0.0 & \underline{-1.7} \end{pmatrix}.$$

- A spin gap is induced by incorporating an anisotropic exchange between Cu1 sites along *y*.
- Modification of J2 produces correct canting of Cu2 spins as refined by neutron diffraction.

[Rousochatzakis *et al.* PRB (2015)]

Overlapping magnon / phonon bands

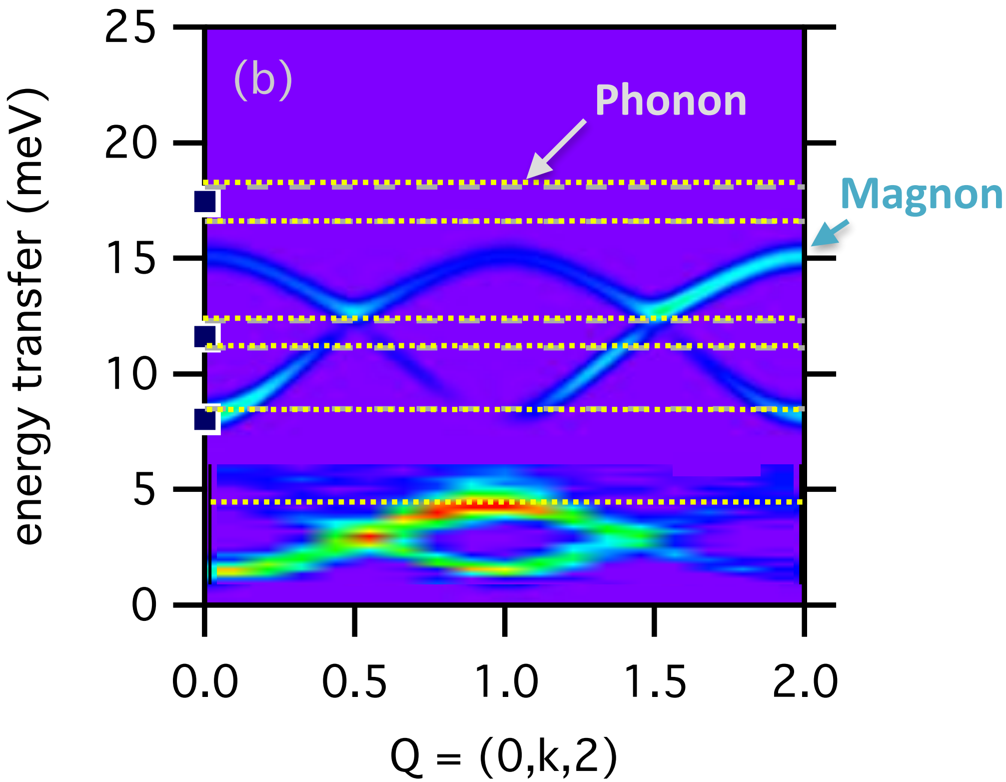

- Overlapping magnon and phonon bands: Possibility for magnon phonon hybridisation.
- Spin-lattice coupling could promote the required anisotropy in the refined magnetic Hamiltonian.
- Polarised inelastic neutron scattering required to reveal signatures of such hybridisation.

Soft phonon dynamics in **b** direction

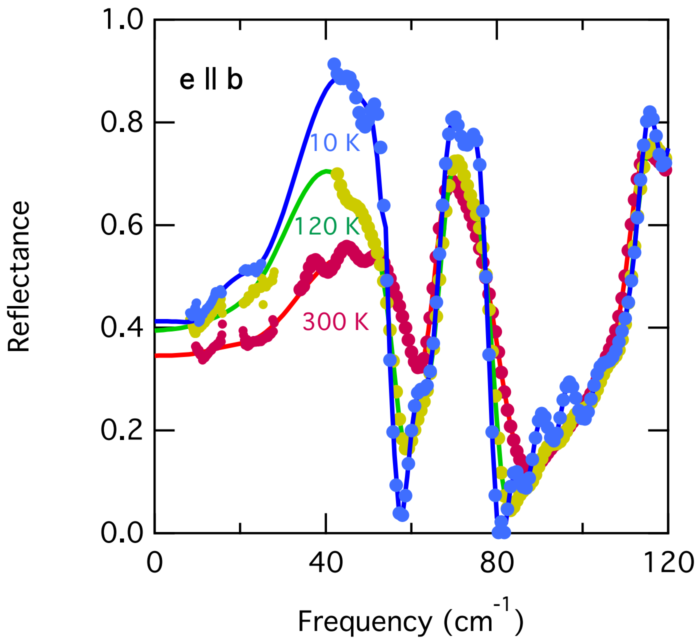

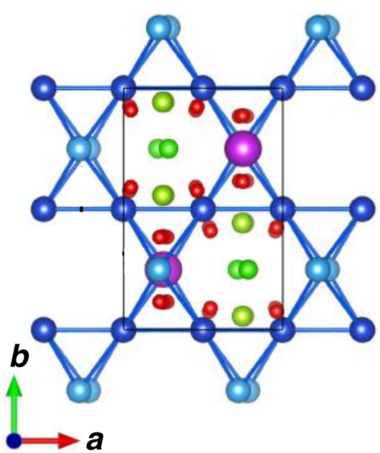

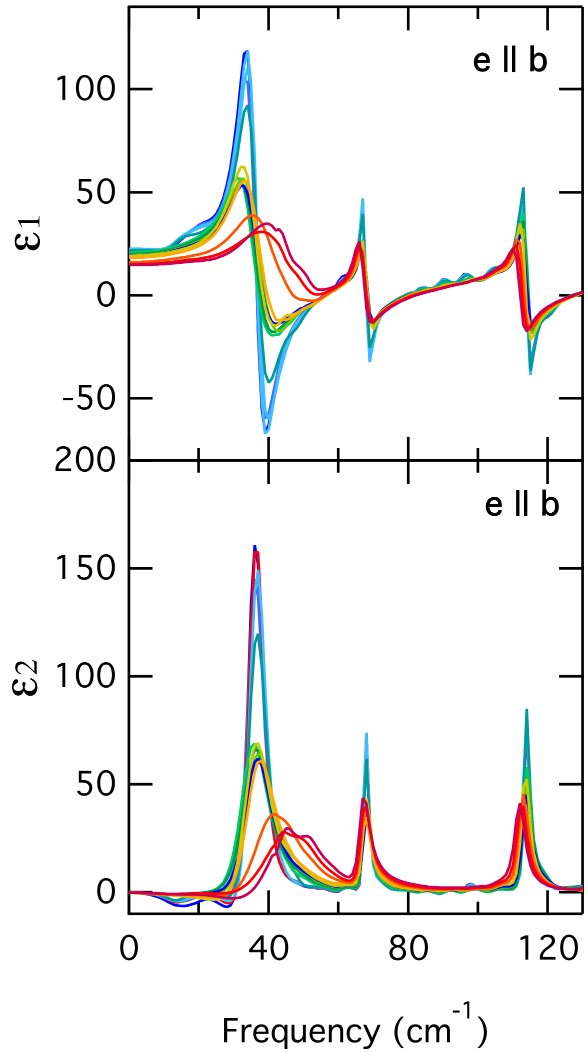

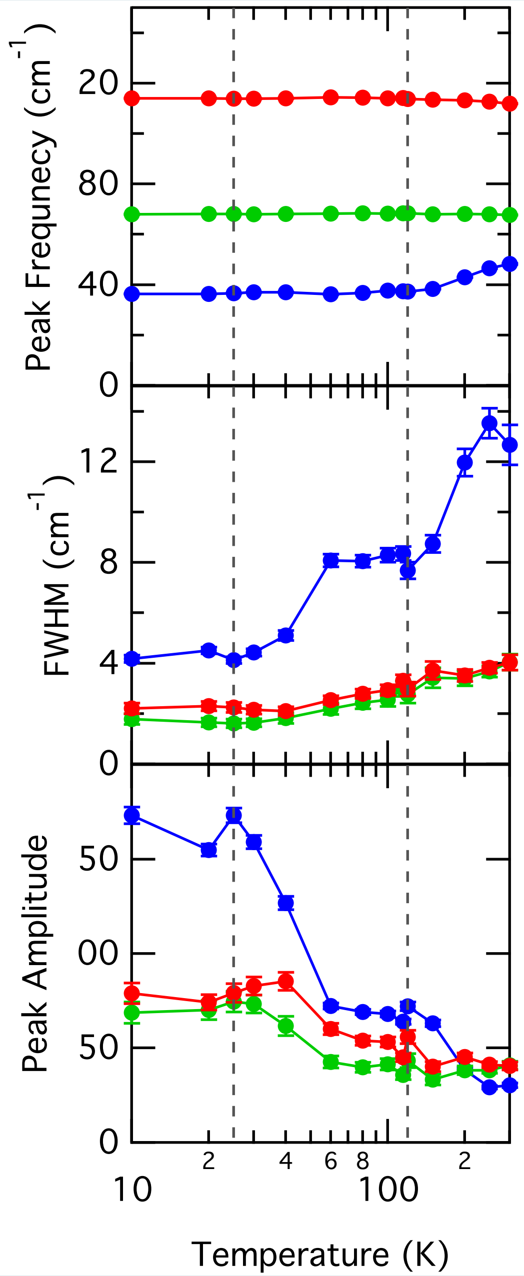

Soft phonon dynamics in **b** direction

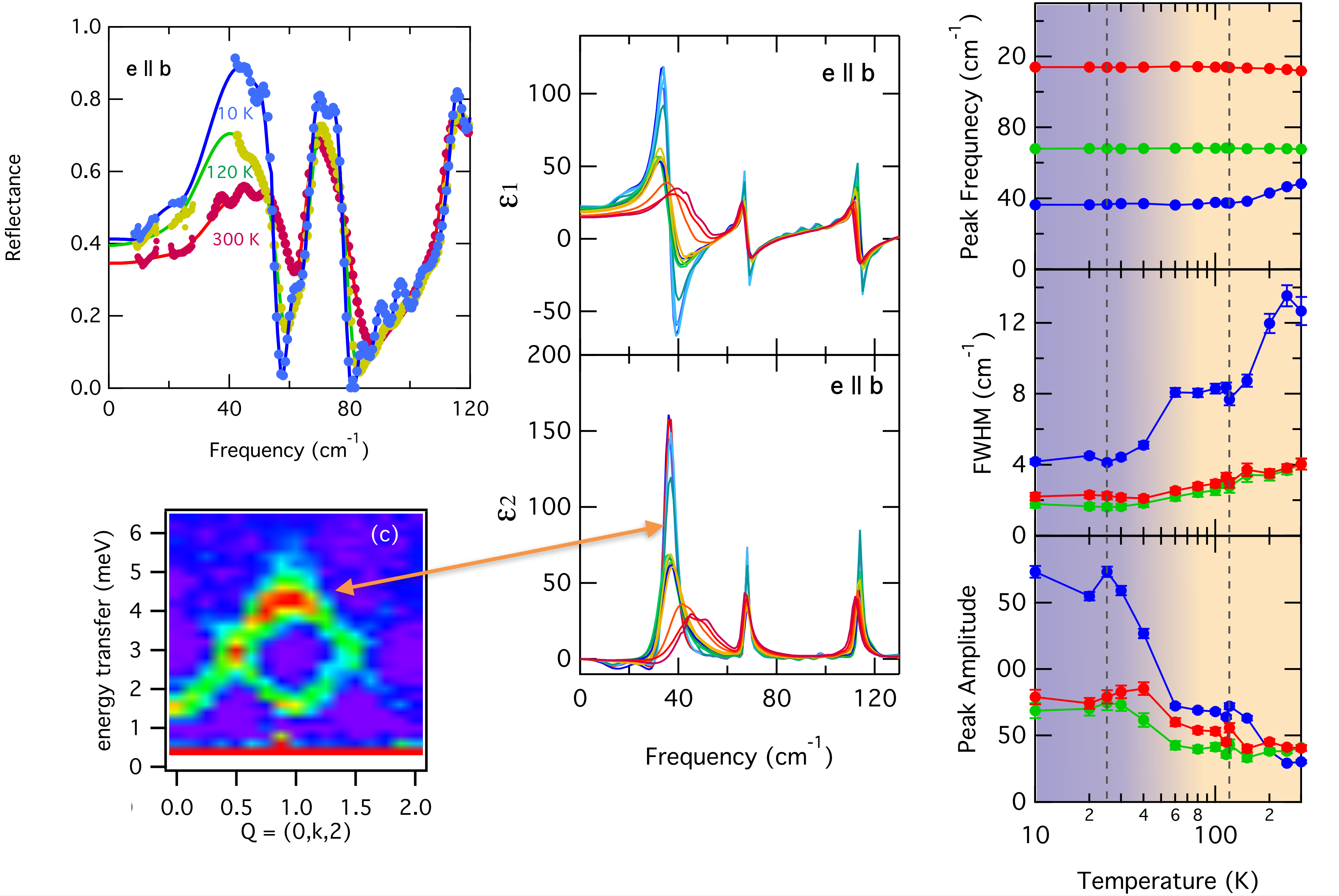

Spontaneous polarisation along **c** for T < T_N

polarisation as a function of magnetic field

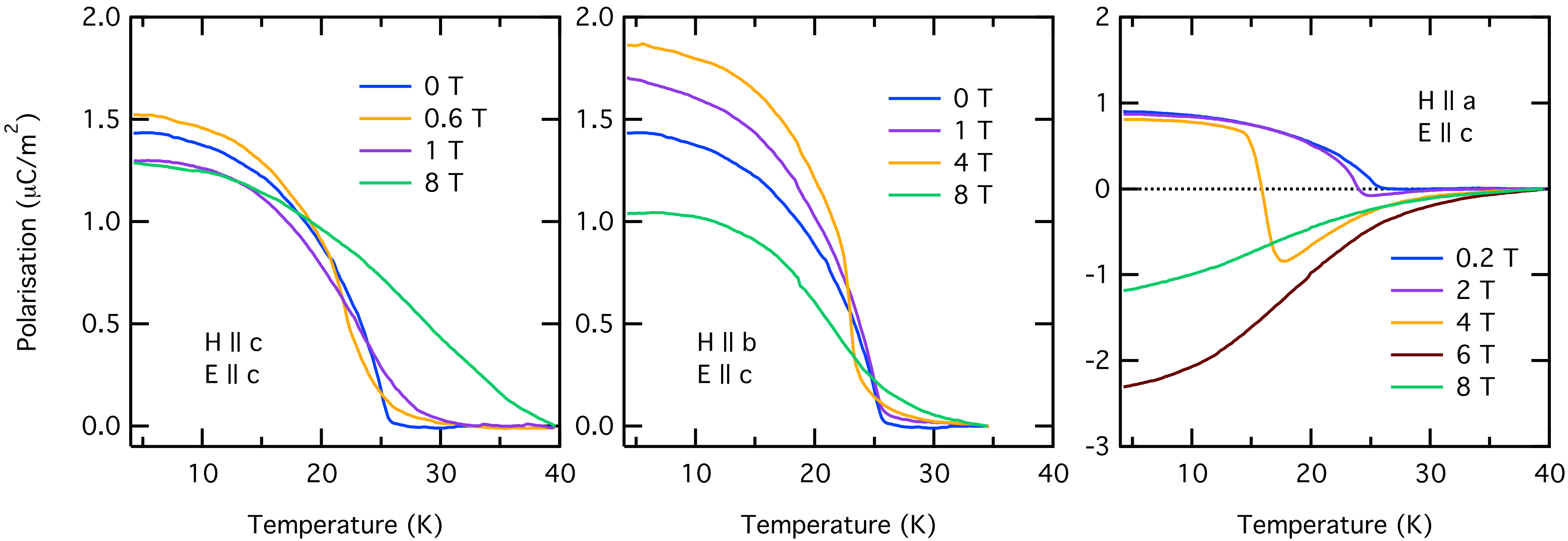

- magnetic point group: *mm′m* supports magneto electric coupling but **does not predict spontaneous polarisation at 0 T**.
- Field dependence is consistent with the of diagonal terms in the ME tensor.
- Presence at 0 T could be explained by magneto electric coupling due to stray fields generated at defects.
- Effect of antiferrfoelectic order?

$$\alpha^{ME} = \begin{pmatrix} 0 & 0 & \alpha_{13}^{ME} \\ 0 & 0 & 0 \\ \alpha_{31}^{ME} & 0 & 0 \end{pmatrix}$$

maximised with HxE

Concluding remarks

- Francisite displays a **novel frustrated magnetic** state:
  - Buckled kagome lattice with nn FM and nnn AFM interactions.
  - Touching soft magnon bands, dispersionless along *l* (quasi 2-D).
  - Spin gap requiring anisotropic exchange modification to Hamiltonian.
  - Supports spontaneous polarisation below TN = 25 K.
- Identification of *Pmmn* -> *Pcmn* transition driven by **antipolar soft mode**:
  - candidate displacive “antiferroelectric”
  - Evidence of spin-lattice coupling.
  - Significance of magntic/antiferroelectric order in domain of multiferroics?
- Still much of the phase space to be explored with many possible substitutions in the chemical formula.